CAPITAL UNIVERSITY OF SCIENCE AND TECHNOLOGY, ISLAMABAD

Impact of Slip Wall on MHD Casson Nanofluid in the Presence of Viscous Dissipation and Thermal Radiation

by

Faiza Anjum

A thesis submitted in partial fulfillment for the degree of Master of Philosophy

in the

Faculty of Computing
Department of Mathematics

2020

Dedicated to my beloved Parents, Siblings and dignified Teachers, who have taught me to work diligently for the things that I aspire to achieve.

CERTIFICATE OF APPROVAL

Impact of Slip Wall on MHD Casson Nanofluid in the Presence of Viscous Dissipation and Thermal Radiation

by

Faiza Anjum

(MMT173035)

THESIS EXAMINING COMMITTEE

S. No.	Examiner	Name	Organization
(a)	External Examiner	Examiner Name	Organization
(b)	Internal Examiner	Examiner Name	Organization
(c)	Supervisor	Supervisor Name	Organization

Dr. Muhammad Sagheer
Thesis Supervisor
August, 2020

Dr. Muhammad Sagheer
Head
Dept. of Mathematics
August, 2020

Dr. Muhammad Abdul Qadir
Dean
Faculty of Computing
August, 2020

Author's Declaration

I, **Faiza Anjum** hereby state that my MPhil thesis titled "**Impact of Slip Wall on MHD Casson Nanofluid in the Presence of Viscous Dissipation and Thermal Radiation**" is my own work and has not been submitted previously by me for taking any degree from Capital University of Science and Technology, Islamabad or anywhere else in the country/abroad.

At any time if my statement is found to be incorrect even after my graduation, the University has the right to withdraw my MPhil Degree.

(Faiza Anjum)

Registration No: MMT173035

Plagiarism Undertaking

I solemnly declare that research work presented in this thesis titled "*Impact of Slip Wall on MHD Casson Nanofluid in the Presence of Viscous Dissipation and Thermal Radiation*" is solely my research work with no significant contribution from any other person. Small contribution/help wherever taken has been dully acknowledged and that complete thesis has been written by me.

I understand the zero tolerance policy of the Higher Education Commission of Pakistan (HEC) and Capital University of Science and Technology towards plagiarism. Therefore, I as an author of the above titled thesis declare that no portion of my thesis has been plagiarized and any material used as referred/cited.

I undertake that if I am found guilty of any formal plagiarism in the above titled thesis even after award of MPhil Degree, the University reserves the right to withdraw/revoke my MPhil degree and that HEC and the University have the right to publish my name on the HEC/University website on which names of students are placed who submitted plagiarized work.

(Faiza Anjum)

Registration No: MMT173035

Acknowledgements

In the name of **Allah**, the Most Gracious and the Most Merciful Alhamdulillah, all praise is due to Allah; we praise Him, seek His help, and ask for His forgiveness. I am thankful to Allah, who supplied me with the courage, the guidance, and the love to complete this research. Also, I cannot forget the ideal man of the world and most respectable personality for whom Allah created the whole universe, Prophet Mohammad (Peace Be Upon Him).

Foremost, I would like to express my sincere gratitude to my supervisor **Dr. Muhammad Sagheer** for his passionate for his patience, motivation, enthusiasm, and immense knowledge. His guidance helped me in all the time of research and writing of this thesis. By working under his supervision, I have not just acquired technical knowledge but also learn about being a good human. I would like to acknowledge CUST for providing me such a favorable environment to conduct this research.

I owe my profound gratitude to **Dr. Shafqat Hussain** for his superb guidance and inexhaustible inspiration throughout this thesis. I am truly thankful to my teachers at Capital University of Science and Technology, **Dr. Rashid Ali**, **Dr. Abdul Rehman Kashif**, **Dr. Dur e Shehwar**, **Dr. Samina Rashid** and **Dr. Muhammad Afzal**.

My heartiest and sincere salutations to my Parents and Siblings, whose love and guidance are with me in whatever I pursue and for providing me unending inspiration. Dear brother **Altaf Hussain**, I wholeheartedly would like to thank you for your intense caring and support in every aspect of my life.

The acknowledgment will surely remain incomplete if I do not express my deep indebtedness and cordial thanks to **Dr. Muhammad Nasir Abrar** for his valuable suggestions, guidance and unending cooperation during my thesis.

Abstract

In this thesis, numerical study of Casson nanofluid in the presence of viscous dissipation, thermal radiation and chemical reaction coefficient past a stretching sheet has been carried out. The non-linear partial differential equations describing the proposed flow problem are reduced to a set of ordinary differential equations via suitable similarity transformations. The shooting method has been used to obtain the numerical results with the help of the computational software MATLAB. The effects of pertinent flow parameters on the non-dimensional velocity, temperature and concentration profiles are presented via tables and graphs. From the results, it has been remarked that the heat transfer rate escalates for the larger values of the radiation parameter for the Casson nanofluid.

Contents

List of Figures

List of Tables

Abbreviations

BVP	Boundary Value Problem
IVP	Initial Value Problem
MHD	Magnetohydrodynamics
ODEs	Ordinary Differential Equations
PDEs	Partial Differential Equations

Symbols

α	Thermal diffusivity
A	Velocity ratio parameter
Bi	Biot number
B_0	Magnetic field parameter
c_p	Specific heat
C	Concentration
C_f	Skin friction coefficient
C_∞	Ambient concentration
δ	Slip parameter
D_T	Thermophoresis diffusion coefficient
D_B	Brownian diffusion coefficient
Ec	Eckert number
η	Dimensionless similarity variable
f	Dimensionless stream function
γ	Casson fluid parameter
k	Thermal conductivity
L_e	Lewis number
μ	Dynamic viscosity of the fluid
M	Magnetic parameter
Nb	Brownian motion parameter
Nt	Thermophoresis parameter
Nu_x	Local Nusselt number
ν	Kinematic viscosity of the fluid

$\phi(\eta)$	Dimensionless concentration
p	Pressure
P_r	Prandtl number
ϕ	Dimensionless concentration function at large values of y
ϕ_w	Dimensionless concentration function at the surface
ρ	Fluid density
R_x	Local Reynolds number
Rd	Thermal radiation parameter
$(\rho)_f$	Density of the fluid
$(\rho c)_f$	Heat capacity of the fluid
$(\rho c)_p$	Heat capacity of a nanoparticle
σ	Electrical conductivity
Sh_x	Local Sherwood number
ψ	Stream function
T_∞	Ambient temperature
T_f	Temperature of a hot fluid
T_w	Uniform temperature over the surface of the plate
$\theta(\eta)$	Dimensionless temperature
T	Temperature
u	Velocity in x-direction
v	Velocity in y-direction

Chapter 1

Introduction

In the last few years, the non-Newtonian fluids attracted the attention of the mathematicians, physicist, engineers, etc., due to their demanding applications of the domestic and industrial usage. In our daily life such applications are all around us, from a morning coffee to an evening bath. Such application includes, toothpaste, paints, gels, lubrication oils, polymers, etc.,. The Navier Stokes equations due to their composite structure, can not effectively describe the flow of non-Newtonian fluids. In the non-Newtonian fluids, the constitutive equations exist much more complex than the Navier Stokes equations. The versatile behavior of fluids does not develop with a single constitutive equation by which all the non-Newtonian fluids can be studied. Some relevant studies on the subject of non-Newtonian fluids can be seen from the list (Wang and Tan [1], Fetecau et al. [2], Cortell [3], Kothandapani and Srinivas [4], Jamil and Fetecau[5], Rashidi et al. [6].)

The study of MHD fluid flow was first established by a Swedish physicist, Alfven [7]. Because of its important applications in engineering processes [8], energy generators [9], planetary and solar plasma fluid dynamics systems [10], magnetic field regulation of material processing device [11], hybrid magnetic propulsion system for space travel [12], industries [13], biomedical sciences [14], many researchers are interested in studying MHD fluid flow. Yih [15] studied the impact of heat and mass transfer for MHD along a continuously moving shear surface.

Modather and Chamkha [16] discussed the time dependent MHD flow past a semi-infinite flat plate. Kesvaiah et al. [17] investigated the MHD flow and heat transfer towards a porous shrinking sheet with temperature bounce and velocity fall. Zheng et al. [18] inspected the magnetic field and thermal radiation on a micropolar fluid near a stagnation point towards a moving surface. Mahmoud and Waheed [19] analyzed the non-uniform fluid flow becacuse of continuously moving flat surface along convective boundary conditions. He used the numerical shooting technique. In the absence of magnetic field, Mustafa et al. [20] discussed the MHD flow with the impact of Joule heating, viscous dissipation and velocity slip. The role of viscous dissipation in different devices plays an important part in normal convection. Yasin et al. [21] discussed the impact of thermal radiation on MHD flow between the horizontal plates. They numerically used the RK-4 approach. Reynolds number, magnetic parameter, Schmidth number, thermophoretic parameter were inspected.

The thickness of the boundary layer is decreased by the rise in radiation parameter. In Sheikholeslami et al's geometry the symbolic impacts of thermophoresis and Brownian motion were observed [22]. Chutia and Deka [23] numerically discussed the heat transfer and steady MHD flow in an electrically protected rectangular pipe in the existence of the attractive field. The inclined magnetic field effects on fluid flow were explored by Singh et al. [24].

1.1 Thesis contribution

In this thesis, a detailed review of [25] is conducted and the results have been imitated by considering the additional impact of slip wall on MHD Casson nanofluid in the presence of viscous dissipation and thermal radiation. In this work, through an appropriate transformation, the obtained PDEs are transform into the dimensionless ODEs. The numerical outcomes are calculated by using the shooting

technique. Using the tables and graphs, different physical parameter effects on the flow and heat conduction are also explained.

1.2 Thesis outline

A compact sketch of the thesis is given as:

1.2.1 Chapter 2

This chapter describes few basic definitions and terminologies. Furthermore some basic laws and dimensionless physical parameters are also included.

1.2.2 Chapter 3

Chapter 3, give full review of [25], which considers MHD stagnation point flow and Casson nanofluid heat transfer past a stretching sheet.

1.2.3 Chapter 4

This chapter extends the model given in [25] by considering the additional impact of slip wall on MHD Casson nanofluid in the presence of viscous dissipation and thermal in the energy equation. Tables and graphs describe the behavior of different physical parameters.

1.2.4 Chapter 5

Chapter 5, gives the conclusion of the entire work and a plan for the future research.

References used in the thesis are mentioned in **Biblography**.

Chapter 2

Preliminaries

Some definitions, basic laws and terminologies would be discussed in the current chapter, which would be used in the next chapters.

2.1 Some Basic Definitions

In this section, some fundamental ideas, laws and terminologies have been presented that will be beneficial for the further discussion [26–32].

2.1.1 Fluid

"A fluid is a substance that deforms continuously under the application of a shear stress, no matter how small the stress may be. Thus fluids comprise of the liquid and gas (or vapour) phases of the physical forms in which matter exists."

2.1.2 Stress

"Stress is a force acted upon a material per unit of its area and is denoted by τ. Mathematically, it can be written as:

$$\tau = \frac{F}{A},$$

where F denotes the force and A represents the area. ”

2.1.2.1 Shear Stress

“It is a type of stress in which the force vector acts parallel to the material surface or the cross section of a material. ”

2.1.2.2 Normal Stress

“It is a type of stress in which the force vector acts perpendicular to the surface of material or the cross section of a material.”

2.1.2.3 Fluid Mechanics

“Fluid mechanics deals with the behaviour of fluids at rest or in motion.”

2.1.3 Fluid Dynamics

“The branch of fluid mechanics that covers the properties of fluid in the state of progression from one place to another is called fluid dynamics.”

2.1.4 Fluid Statics

“Fluid static is the branch of fluid mechanics, that deals with a fluid and its characteristics at the constant position.”

2.1.5 Mass Transfer

“Mass transfer is the total movement of mass from one place to another.”

2.1.6 Heat Transfer

"It is the energy transfer due to temperature difference. At the point when there is a temperature contrast in a medium or between media, heat transfer must take place. Heat transfer is normally conducted from a high temperature region to a low temperature. For example, heat is transferred from stove to the cooking pan."

2.1.7 Conduction

"Conduction is the process in which heat is transferred through the material between the objects that are in physical contact. For example,

- picking up a hot cup of tea,
- after a car is turned on, the engine becomes hot,
- a radiator is a good example of conduction."

2.1.8 Convection

"Convection is a mechanism in which heat is transferred through fluids (gases or liquids) from a hot place to a cool place. For example,

- macaroni rising and falling in a pot of boiling water,
- streaming cup of hot tea. The steam is showing heat transferred into the air. "

2.1.9 Thermal Radiation

"The process by which heat is transferred from a body by virtue of its temperature, without the aid of any intervening medium is called thermal radiation. For example, toasters use thermal radiations emitted by its element to toast bread."

2.1.10 Boundary Layer

"Viscous effects are particularly important near the solid surfaces, where the strong interactions of the fluid with molecules of the solid causes the relative velocity between the fluid and the solid to become almost zero for a stationary surface. Therefore, the fluid velocity in the region near the wall must reduce to zero. This is called no slip condition. In this condition, there is no relative motion between the fluid and the solid surface at their point of contact. It follows that the flow velocity varies with distance from the wall; from zero at the wall to its full value some distance away, so that significant velocity gradients are established close to the wall. In most cases this region is thin (compared to typical body dimension), and is called boundary layer."

2.2 Conservation Laws [33]

"Several conservation laws such as the laws of conservation of mass, conservation of energy and conservation of momentum are of great use for the research community. Historically, the conservation laws were first applied to a fixed quantity of matter called a closed system or just a system, and then extended to regions in space called control volumes. The conservation relations are also called balance equations since any conserved quantity must balance during a process."

2.2.1 Conservation of Mass

"Law of conversation of mass states that mass can neither be created nor be destroyed in a chemical reaction. The conservation of mass relation for a closed system undergoing a change is expressed as:

$$m_{sys} = \text{constant},$$

or

$$\frac{dm_{\text{sys}}}{dt} = 0,$$

which is an obvious statement that the mass of the system remains constant during a process. For a control volume (CV), mass balance is expressed in the rate form as:

$$m_{in} - m_{out} = \frac{dm_{CV}}{dt}$$

where m_{in} and m_{out} are the total rates of mass flow into and out of the control volume, respectively, and $\frac{dm_{CV}}{dt}$ is the rate of change of mass within the control volume boundaries. In fluid mechanics, the conservation of mass relation written for a differential control volume is usually called the continuity equation."

2.2.2 Conservation of Momentum

"The product of the mass and the velocity of a body is called the linear momentum or just the momentum of the body, and the momentum of a rigid body of mass m moving with a velocity $\overrightarrow{V}$ is $m\overrightarrow{V}$. Newtons second law states that the acceleration of a body is proportional to the net force acting on it and is inversely proportional to its mass, and that the rate of change of the momentum of a body is equal to the net force acting on the body. Therefore, the momentum of a system remains constant when the net force acting on it is zero, and thus the momentum of such systems is conserved. This is known as the conservation of momentum principle."

2.2.3 Conservation of Energy

"This law states that energy can neither be created nor be destroyed, rather it can only be transferred from one form to another. Energy can be transferred to or from a closed system by heat or work, and the conservation of energy principle requires that the net energy transfer to or from a system during a process be equal to the change in energy content of the system. Control volumes involve energy

transfer via mass flow also, and the conservation of energy principle, also called the energy balance, is expressed as:

$$\mathtt{E}_{in} - \mathtt{E}_{out} = \frac{dE_{CV}}{dt},$$

where $\mathtt{E}_{in}$ and $\mathtt{E}_{out}$ are the total rates of energy transfer into and out of the control volume, respectively, and $\frac{dE_{CV}}{dt}$ is the time rate of change of energy within the control volume boundaries. In fluid mechanics, we usually limit our consideration to mechanical forms of energy only."

2.3 Flow [30]

"It is the deformation of the material under the influence of different forces. If the deformation increase is continuous without any limit, then the process is known as flow."

2.3.1 Compressible and Incompressible Flows

"Flow in which variations in density are negligible is termed as incompressible otherwise it is called compressible. The most common example of compressible flow is the flow of gases, while the flow of liquids may frequently be treated as incompressible.

Mathematically, for compressible flow:

$$\frac{D\rho}{Dt} = 0,$$

where ρ denotes the fluid density and $\frac{D}{Dt}$ is the material derivative given by;

$$\frac{D}{Dt} = \frac{\partial}{\partial t} + \mathbf{v}.\bigtriangledown,$$

where $\mathbf{v}$ denotes the velocity of flow and $\bigtriangledown$ is the differential operator. In Cartesian coordinate system, $\bigtriangledown$ is given as:

$$\nabla = \frac{\partial}{\partial x}\widehat{i} + \frac{\partial}{\partial y}\widehat{j} + \frac{\partial}{\partial z}\widehat{k}."$$

2.3.2 Uniform and Non-uniform Flows

"The flow is said to be uniform if the magnitude and direction of flow velocity are the same at every point and the flow is said to be non-uniform if the velocity is not the same at each point of flow, at a given instant."

2.3.3 Steady and Unsteady Flows

"A flow is said to be steady flow in which the fluid properties do not change with time at a specific point,

$$\frac{\partial \lambda}{\partial t} = 0,$$

where λ is any fluid property. A flow is said to be unsteady in which the fluid properties change with time, i.e "

$$\frac{\partial \lambda}{\partial t} \neq 0.$$

2.3.4 Laminar and Turbulent Flows

"A flow is laminar in which the fluid particles move in smooth layers or laminar and a turbulent in which the fluid particles rapidly mix as they move along due to random three-dimensional velocity fluctuations. "

2.3.5 Viscosity

"It is the property of the fluid that resists the fluid flow. In other words, a fluid viscosity is that characteristic which measures the amount of resistance to the shear stress. It is denoted by μ and mathematically, it can be written as:

$$\text{Viscosity} = \mu = \frac{\text{shear stress}}{\text{rate of shear strain}}.\text{"}$$

2.3.6 Kinematic Viscosity

"The ratio of the dynamic viscosity to the density of fluid is said to be kinematic viscosity. Symbolically, it can be written as ν and mathematically, it is expressed as:

$$\nu = \frac{\mu}{\rho},$$

where μ and ρ denote the dynamic viscosity and the density respectively. The dimension of kinematic viscosity is given by $[\frac{L^2}{T}]$. "

2.4 Newtonian and Non-Newtonian Fluids

"Newtonian fluids fulfill Newtons law of viscosity which can be written mathematically as:

$$\tau_{xy} = \mu\left(\frac{du}{dy}\right),$$

where

$\mu =$ Dynamic viscosity,
$\tau_{xy} =$ Shear stress $= \frac{F}{A}$,
$\frac{du}{dy} =$ Rate of shear deformation.

The most common examples of Newtonian fluid are water, glycerol.
The fluids, which do not obey the Newtons law of viscosity are known as non-Newtonian fluids. For such fluids,

$$\tau_{xy} = k\left(\frac{du}{dy}\right)^n,$$

where

k is the flow consistency index,
$\frac{du}{dy}$ is shear rate,
n is flow behaviour index.

For $n = 1$ with $k = \mu$, the above equation reduces to the Newtons's law of viscosity. Paints, blood, biological fluids and polymer melts are good examples of non-Newtonian fluids."

2.5 Viscous Dissipation

"The process in which the work done by fluid is converted into heat is called viscous dissipation. In thermodynamics, dissipation is the result of an irreversible process that takes place in homogeneous thermodynamic systems. A dissipative process is a process in which energy (internal, bulk flow kinetic, or system potential) is transformed from some initial form to some final form; the capacity of the final form to do mechanical work is less than that of the initial form. For example, heat transfer is dissipative because it is a transfer of internal energy from a hotter body to a colder one. Following the second law of thermodynamics, the entropy varies with temperature (reduces the capacity of the combination of the two bodies to do mechanical work), but never decreases in an isolated system."

2.6 Thermal Conductivity

"Thermal conductivity k is the property of a material related to its ability to transfer heat. Mathematically,

$$k = \frac{q \bigtriangledown l}{S \bigtriangledown T},$$

where q is the heat passing through a surface area S and the effect of a temperature difference $\bigtriangledown T$ over a distance is $\bigtriangledown l$. Here l, S and $\bigtriangledown T$ all are assumed to be of

unit measurement. In SI unit of thermal conductivity is watt per meter kelvin and its dimension is $[MLT^{-1}\theta^{-1}]$."

2.7 Thermal Diffusivity

"Thermal diffusivity is material's property which identifies the unsteady heat conduction. Mathematically, it can be written as:

$$\alpha = \frac{k}{\rho C_p},$$

where k, ρ and C_p represent the thermal conductivity of material, the density and the specific heat capacity. In SI system unit and dimension of thermal diffusivity are $m^2 s^{-1}$ and $[LT^{-1}]$ respectively."

2.8 Dimensionless Parameters [31]

Following section reflects the definitions of certain dimensionless used in this study.

2.8.1 Reynolds Number

"This number expresses the ratio of the fluid inertial force to that of molecular friction (viscosity). It determines the character of the flow (laminar, turbulent and transient flows). Mathematically, it can be write as:

$$R_e = \frac{u_0 H}{\nu},$$

where H is characteristic length, u_0 the flow velocity and ν is the kinematic viscosity."

2.8.2 Eckert Number

"It is the dimensionless number used in continuum mechanics. It describes the relation between flows and the boundary layer enthalpy difference and it is used for characterized heat dissipation. Mathematically,

$$E_c = \frac{u^2}{C_p \bigtriangledown T},$$

where u is local flow velocity, C_p is the specific heat and $\bigtriangledown T$ is the difference between wall temperature."

2.8.3 Prandtl Number

"This number expresses the ratio of the momentum diffusivity (viscosity) to the thermal diffusivity. Mathematically, it can be written as:

$$P_r = \frac{\nu}{\alpha} = \frac{\mu/\rho}{k/\rho C_p} = \frac{\mu C_p}{k},$$

where ν represents the kinematic viscosity and α denotes the thermal diffusivity. It characterizes the physical properties of a fluid with convective and diffusive transfers."

2.8.4 Schmidt Number

"It is the ratio between kinematic viscosity ν and molecular diffusion D. It is denoted by S_c and mathematically we can write it as:

$$S_c = \frac{\nu}{D},$$

where ν is the kinematic viscosity and D is the mass diffusivity."

2.8.5 Skin Friction Coefficient

"Skin friction co-efficient occurs between the fluid and solid surface which leads to slow down the motion of fluid. The skin friction co-efficient is defined as:

$$C_f = \frac{2\tau_w}{\rho U^2},$$

where τ_w denotes the wall shear stress, ρ the density and U the free-stream velocity."

2.8.6 Nusselt Number

"It is the ratio of the convective to the conductive heat heat transfer to the boundary. Mathematically,

$$Nu = \frac{hL}{k},$$

where h stands for convective heat transfer, L stands for the characteristic length and k stands for the thermal conductivity."

2.8.7 Sherwood Number

"It is the non-dimensional quantity which shows the ratio of the mass transport by convection to the transfer of mass by diffusion. Mathematically,

$$Sh = \tfrac{kL}{D},$$

where L is characteristics length, D is the mass diffusivity and k is the mass transfer co-efficient."

Chapter 3

Impact of Slip Wall on MHD Casson Nanofluid

3.1 Introduction

This chapter explains the Casson nanofluid flow over a linear stretching sheet along with the slip wall. Mainly, the analysis of heat and mass transfer in the presence of Brownian motion and the thermophoretic diffusion effect is performed. The obtained PDEs are transformed into the dimensionless ODEs with the help of transformation. To achieve numerical solution for the considered model, shooting technique has been recruited. For the velocity, temperature, and concentration profiles, the numerical computations are conducted. In addition, physical quantities of absorption like; skin friction, local Nusselt and Sherwood number are also shown graphically. A detailed review work of Ibrahim and Makinde [25] has been presented in this chapter.

3.2 Mathematical Modeling

Consider the 2-D stagnation point flow of MHD Casson fluid over an stretching sheet under the impact of slip wall. Magnetic field of strength B_0 is applied

perpendicular to the fluid motion. Additionally, the impacts of Brownian motion and thermophoretic diffusion are also considered. Furthermore, the equations of energy and mass transport are known to determine the profiles of temperature and concentration respectively. The Cartesian coordinate system is regarded in such a way that x-axis is taken along the stretching plate and y- axis is normal to the plate.

The stretching and slip velocities at the boundary are taken as $U_w(x) = ax$ and $U_{slip} = \left(\mu_B + \frac{P_y}{\sqrt{2\pi_c}}\right)\frac{\partial u}{\partial y}$ respectively, where P_y denotes the yield stress, T_w is the surface temperature, μ_B is the plastic dynamic viscosity, π_c represents the critical value of product, $U_\infty = bx$, T_∞ and C_∞ represent the free stream velocity, temperature and concentration. The physical model is dispensed with graphical representation in Figure 3.1.

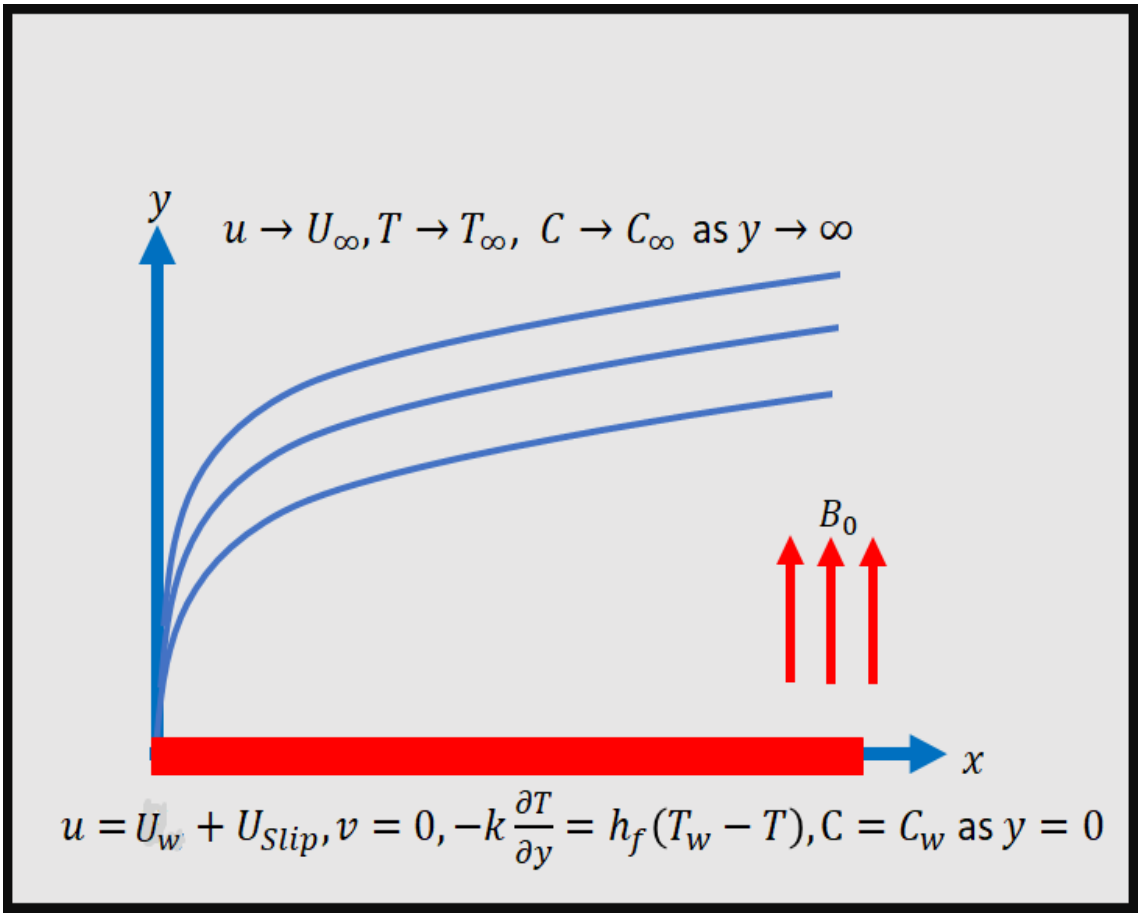

FIGURE 3.1: Physical representation of the problem

3.2.1 Governing equations

The governing boundary layer equations are shown as follows for the two dimensional incompressible Casson nanofluid:

$$\frac{\partial u}{\partial x} + \frac{\partial v}{\partial y} = 0, \tag{3.1}$$

$$u\frac{\partial u}{\partial x} + v\frac{\partial u}{\partial y} = \nu\left(1+\frac{1}{\gamma}\right)\frac{\partial^2 u}{\partial y^2} + U_\infty\frac{\partial U_\infty}{\partial x} + \frac{\sigma B_0^2}{\rho_f}(U_\infty - u), \tag{3.2}$$

$$u\frac{\partial T}{\partial x} + v\frac{\partial T}{\partial y} = \alpha\frac{\partial^2 T}{\partial y^2} + \Gamma\left[D_B\frac{\partial C\partial T}{\partial y\partial y} + \frac{D_T}{T_\infty}\left(\frac{\partial T}{\partial y}\right)^2\right], \tag{3.3}$$

$$u\frac{\partial C}{\partial x} + v\frac{\partial C}{\partial y} = D_B\frac{\partial^2 C}{\partial y^2} + \frac{D_T\partial^2 T}{T_\infty\partial y^2}. \tag{3.4}$$

The required boundary conditions are:

$$\left.\begin{aligned}
&\textbf{Wall conditions } (y=0)\textbf{:}\\
&u = U_w(x) + U_{Slip} \rightarrow u = ax + \left(\mu_B + \frac{P_y}{\sqrt{2\pi_c}}\right)\frac{\partial u}{\partial y}, \quad v = 0,\\
&-k\frac{\partial T}{\partial y} = h_f(T_f - T), \quad C = C_w.\\
&\textbf{Free stream conditions } (y\rightarrow\infty)\textbf{:}\\
&u \rightarrow U_\infty = bx, \quad v = 0, \quad T \rightarrow T_\infty, \quad C \rightarrow C_\infty.
\end{aligned}\right\} \tag{3.5}$$

Here, u and v are components of velocity in the x and y direction respectively, γ denotes the Casson parameter, ρ_f is the fluid density, T represents the temperature, α is the thermal diffusivity, C is the concentration parameter, k denotes the thermal conductivity, h_f denotes the coefficient of heat transfer and a and b are positive constant.

3.2.2 Similarity Transformation

The following similarity variables for translation of PDEs into ODEs have been added here.

$$\left.\begin{aligned} \eta &= y\sqrt{\frac{a}{\nu}}, \qquad \psi = \sqrt{a\nu}xf(\eta), \\ \theta(\eta) &= \frac{T-T_\infty}{T_w-T_\infty}, \quad \phi(\eta) = \frac{C-C_\infty}{C_w-C\infty}. \end{aligned}\right\} \tag{3.6}$$

Following are some significant derivatives essential for further derivation.

- $u = \dfrac{\partial\psi}{\partial y}, \qquad v = -\dfrac{\partial\psi}{\partial x},$
- $\psi = \sqrt{a\nu}xf(\eta), \qquad \eta = y\sqrt{\dfrac{a}{\nu}},$
- $$\begin{aligned} u &= \frac{\partial\psi}{\partial y} \\ &= \frac{\partial}{\partial y}\left[\sqrt{a\nu}xf(\eta)\right] \\ &= \sqrt{a\nu}xf'\frac{\partial\eta}{\partial y} \\ &= axf'. \end{aligned} \tag{3.7}$$
- $$\begin{aligned} v &= -\frac{\partial\psi}{\partial x} \\ &= -\frac{\partial}{\partial x}\left[\sqrt{a\nu}xf(\eta)\right] \\ &= -\sqrt{a\nu}\left[(1)f(\eta) + xf'\frac{\partial\eta}{\partial x}\right] \\ &= -\sqrt{a\nu}f(\eta). \qquad \because \left(\frac{\partial\eta}{\partial x} = 0\right) \end{aligned} \tag{3.8}$$
- $$\begin{aligned} u &= axf' \\ \frac{\partial u}{\partial x} &= af' + axf''\frac{\partial\eta}{\partial x} \\ &= af' \\ \frac{\partial u}{\partial y} &= axf''\frac{\partial\eta}{\partial y} \\ &= a^{\frac{3}{2}}\frac{x}{\sqrt{\nu}}f'' \end{aligned} \tag{3.9}$$
- $\dfrac{\partial^2 u}{\partial x^2} = af''\dfrac{\partial\eta}{\partial x}$

- $$\frac{\partial^2 u}{\partial y^2} = a^{\frac{3}{2}} \frac{x}{\sqrt{\nu}} f''' \frac{\partial \eta}{\partial y}$$
$$= \frac{a^2 x}{\nu} f'''$$
- $$v = -\sqrt{a\nu} f. \tag{3.10}$$
- $$\frac{\partial v}{\partial x} = -\sqrt{a\nu} f' \frac{\partial \eta}{\partial x}$$
$$\frac{\partial v}{\partial x} = 0 \tag{3.11}$$
- $$\frac{\partial^2 v}{\partial x^2} = 0 \tag{3.12}$$
- $$\frac{\partial v}{\partial y} = -\sqrt{a\nu} f' \frac{\partial \eta}{\partial y}$$
$$= -\sqrt{a\nu} f' \sqrt{\frac{a}{\nu}} \qquad \because \left(\frac{\partial \eta}{\partial y} = \sqrt{\frac{a}{\nu}}\right)$$
$$= -af' \tag{3.13}$$
- $$\frac{\partial^2 v}{\partial y^2} = af'' \frac{\partial \eta}{\partial y}$$
$$= af'' \sqrt{\frac{a}{\nu}}$$
$$= \frac{a^{\frac{3}{2}}}{\sqrt{\nu}} f''. \tag{3.14}$$

Verification of continuity equation (3.1) is straightforwardly done as follows:

$$\frac{\partial u}{\partial x} + \frac{\partial v}{\partial y} = af' + (-af)$$
$$= af' - af'$$
$$\frac{\partial u}{\partial x} + \frac{\partial v}{\partial y} = 0. \tag{3.15}$$

For the conversion of momentum equation (3.2), we proceed as follows:

$$u\frac{\partial u}{\partial x} + v\frac{\partial u}{\partial y} = axf'\left(af'\right) + \left(-\sqrt{a\nu} f\right)\left(\frac{a^{\frac{3}{2}}}{\nu} f''\right)$$

- $$u\frac{\partial u}{\partial x} + v\frac{\partial u}{\partial y} = a^2 x (f')^2 - a^2 x f''$$
- As $U_\infty = bx$,

$$\therefore \frac{\partial U\infty}{\partial x} = b.$$

Putting above equations in (3.2)

$$a^2x(f')^2 - a^2xff'' = \nu\left(1+\frac{1}{\gamma}\right)\frac{a^2x}{\nu}f''' + bx.b + \frac{\sigma B_0^2}{\rho_f}\left(bx - axf'\right)$$
$$a^2x(f')^2 - a^2xff'' = \left(1+\frac{1}{\gamma}\right)a^2xf''' + b^2x + \frac{\sigma B_0^2}{\rho_f}bx - \frac{\sigma B_0^2}{\rho_f}axf' \tag{3.16}$$

The dimensionless form of (3.2) is as follows:

$$a^2xf'^2 - a^2xff'' = \left(1+\frac{1}{\gamma}\right)a^2xf''' + b^2x + \frac{\sigma B_0^2}{\rho_f}bx - \frac{\sigma B_0^2}{\rho_f}axf' \tag{3.17}$$

Dividing each term of (3.17) by a^2x we get,

$$(f')^2 - ff'' = \left(1+\frac{1}{\gamma}\right)f''' + \frac{b^2}{a^2} + \frac{\sigma B_0^2 b}{a^2\rho_f} - \frac{\sigma B_0^2}{a\rho_f f}f'$$
$$(f')^2 - ff'' = \left(1+\frac{1}{\gamma}\right)f''' + \left(\frac{b}{a}\right)^2 + \frac{\sigma B_0^2}{a\rho_f}\left(\frac{b}{a} - f'\right)$$
$$\left(1+\frac{1}{\gamma}\right)f''' + ff'' - (f')^2 + A^2 + M(A - f') = 0, \tag{3.18}$$

where

$$\left(A = \frac{b}{a},\ M = \frac{\sigma B_0^2}{a\rho_f}\right)$$

For the verification of energy equation (3.3), we proceed as follows: As

- $$\theta(\eta) = \frac{T - T_\infty}{T_w - T_\infty}$$
  $$T = T\infty + (T_w - T_\infty)\theta(\eta)$$
  $$\frac{\partial T}{\partial x} = 0 + (T_w - T_\infty)\theta'$$
  $$\frac{\partial T}{\partial x} = 0 \qquad \because \left(\frac{\partial \eta}{\partial x} = 0\right)$$
- $$\frac{\partial T}{\partial y} = 0 + (T_w - T_\infty)\theta'\frac{\partial \eta}{\partial y}$$
  $$\frac{\partial \eta}{\partial y} = \sqrt{\frac{a}{\nu}}(T_w - T\infty)\theta'$$

- $$\frac{\partial^2 T}{\partial y^2} = \sqrt{\frac{a}{\nu}}(T_w - T\infty)\theta'' \frac{\partial \eta}{\partial y}$$
$$= \frac{a(T_w - T_\infty)}{\nu}\theta'' \qquad \because \left(\frac{\partial \eta}{\partial y} = \sqrt{\frac{a}{\nu}}\right) \tag{3.19}$$

Also,

$$\phi(\eta) = \frac{C - C_\infty}{C_w - C_\infty} \tag{3.20}$$

- $C = C_\infty + (C_w - C_\infty)\phi(\eta)$
$\frac{\partial C}{\partial x} = 0 + (C_w - C_\infty)\phi' \frac{\partial \eta}{\partial x}$
$\frac{\partial C}{\partial x} = 0$
- $\frac{\partial C}{\partial y} = 0 + (C_w - C_\infty)\phi' \frac{\partial \eta}{\partial y}$
$= (C_w - C_\infty)\phi' \sqrt{\frac{a}{\nu}}$
$= \sqrt{\frac{a}{\nu}}\,(C_w - C_\infty)\phi'$
- $\frac{\partial^2 C}{\partial y^2} = \sqrt{\frac{a}{\nu}}\,(C_w - C_\infty)\phi'' \frac{\partial \eta}{\partial y}$
$= \frac{a}{\nu}(C_w - C_\infty)\phi''.$ (3.21)

Putting all converted expressions in (3.3), we get

$$0 + \left(- \sqrt{\frac{a}{\nu}} f \right) \sqrt{\frac{a}{\nu}}(T_w - T_\infty)\theta' = \alpha \frac{a(T_w - T_\infty)}{\nu}\theta''$$
$$+ \Gamma \left[D_B \sqrt{\frac{a}{\nu}}(C_w - C_\infty)\phi' \sqrt{\frac{a}{\nu}}(T_w - T\infty)\theta' \right]$$
$$+ \Gamma \left[\frac{DT}{T_\infty} \sqrt{\frac{a}{\nu}}(T_w - T_\infty)\theta'^{\,2} \right]$$
$$- a(T_w - T_\infty) f\theta' = \alpha \frac{a(T_w - T_{infty})}{\nu}\theta''$$
$$+ \Gamma \left[\frac{D_B a}{\nu}(C_w - C\infty)(T_w - T_\infty)\phi'\theta' + \frac{aD_T}{\nu T_{infty}}(T_w - T_\infty)^2(\theta')^2 \right]$$
$$- a(T_w - T_\infty) f\theta' = \alpha \frac{a(T_w - T_\infty)}{\nu}\theta''$$
$$+ \Gamma \frac{(\rho C)_p}{(\rho C)_f} \frac{a}{\nu} D_B (C_w - C_\infty)(T_w - T\infty)\phi'\theta'$$
$$+ \frac{(\rho C)_p}{(\rho C)_f} \frac{a}{\nu} \frac{D_T}{D_\infty}(T_w - T_\infty)^2 \theta'^2. \qquad \because \left(\Gamma = \frac{(\rho C)_p}{(\rho C)_f}\right)$$

Multiply each term by

$$\frac{\nu}{\alpha\, a(T_w - T_\infty)}$$

$$-\frac{\nu}{\alpha} f\theta' = \theta'' + \frac{(\rho C)_p}{(\rho C)_f \alpha} D_B (C_w - C_\infty)\phi'\theta' + \frac{(\rho C)_p}{(\rho C)_f \alpha}\frac{D_T}{T_\infty}(T_w - T_\infty)\theta'^2, \quad (3.22)$$

as

$$Pr = \frac{\nu}{\alpha},$$

$$-Prf\theta' = \theta'' + \frac{(\rho C)_p}{\alpha(\rho C)_f} D_B (C_w C_\infty)\phi'\theta' + \frac{(\rho C)_p}{(\rho C)_f \alpha}\frac{D_T}{T_\infty}(T_w - T_\infty)\theta'^2, \quad (3.23)$$

$$-\frac{\nu}{\nu} Prf\theta' = \frac{\nu}{\nu}\theta'' + \frac{\nu}{\nu}\frac{(\rho C)_p}{\alpha(\rho C)_f} D_B (C_w C_\infty)\phi'\theta' + \frac{\nu}{\nu}\frac{(\rho C)_p}{(\rho C)_f \alpha}\frac{D_T}{T_\infty}(T_w - T_\infty)\theta'^2,$$

$$-Prf\theta' = \theta'' + Pr\frac{(\rho C)_p}{\nu(\rho C)_f} D_B (C_w - C_\infty)\phi'\theta' + Pr\frac{(\rho C)_p}{(\rho C)_f \nu}\frac{D_T}{T_\infty}(T_w - T_\infty)\theta'^2,$$

$$-Prf\theta' = \theta'' + PrNb\phi'\theta' + PrNt(\theta')^2, \quad (3.24)$$

$$\theta'' + Prf\theta' + PrNb\phi'\theta' + PrNt(\theta')^2 = 0, \quad (3.25)$$

where

$$Nb = \frac{(\rho C)_p}{(\rho C)_f \nu} D_B (C_w - C_\infty),$$

$$Nt = \frac{(\rho C)_p}{(\rho C)_f \nu} D_T (T_w - T_\infty)$$

Similarly the following procedure elaborates the conversion of concentration equation. Using above converted expression in (3.4)

$$0 + (-\sqrt{a\nu}f).\sqrt{\frac{a}{\nu}}f(C_w - C_\infty)\phi' = D_B\frac{a(C_w - C_\infty)}{\nu}\phi'' + \frac{D_T}{T_\infty}a\frac{T_w - T_\infty}{\nu}\theta'',$$
$$-\sqrt{a\nu\frac{a}{\nu}}(C_w - C_\infty)f\phi' = \frac{D_B}{\nu}a(C_w - C_\infty)\phi'' + \frac{D_T\, a}{T_\infty\,\nu}(T_w - T_\infty)\theta'',$$
$$-a(C_w - C_\infty)f\phi' = \frac{D_B}{\nu}a(C_w - C_\infty)\phi'' + \frac{D_T\, a}{T_\infty\,\nu}(T_w - T_\infty)\theta''.$$

Multiplying each term by

$$\frac{\nu}{aD_B(C_w - C_\infty)}$$

$$-\frac{\nu}{D_B}f\phi' = \phi'' + \frac{D_T}{D_B\,T_\infty}\frac{T_w - T_\infty}{C_w - C_\infty}\theta'' \tag{3.26}$$

- $Le\ Pr = \dfrac{\alpha}{D_B}\dfrac{\nu}{\alpha}$
- $Le\ Pr = \dfrac{\nu}{D_B}$ (3.27)
- $\dfrac{Nt}{Nb} = \dfrac{(\rho C)_p\, D_T(T_w - T_\infty)}{(rhoC)_f}\nu\, T_\infty \div \dfrac{(\rho C)_p\, D_B(\phi_w - \phi_\infty)}{(rhoC)_f}\nu$ (3.28)

$$= \frac{(\rho C)_p\, D_T(T_w - T_\infty)}{(rhoC)_f}\nu\, T_\infty \cdot \frac{(\rho C)_f\,\nu}{(\rho C)_p}D_B(\phi_w - \phi_\infty)$$

$$= \frac{D_T(T_w - T_\infty)}{D_B\,T_\infty(C_w - C\infty)} \tag{3.29}$$

Putting (3.27) and (3.28) in (3.26) we get,

$$-\frac{\nu}{D_B}f\phi' = \phi'' + \frac{D_T(T_w - T_\infty)}{D_BT_\infty(C_w - C_\infty)}\theta''$$

$$-Le\ Pr\ f\ \phi' = \phi'' + \frac{Nt}{Nb}\theta''$$

$$\phi'' + Le\ Pr\ f\ \phi' + \frac{Nt}{Nb}\theta'' = 0. \tag{3.30}$$

Finally, the ODEs describing the proposed flow problem can be re-collected in the following system.

$$\left(1+\frac{1}{\gamma}\right)f'''+ff''-(f')^2+A^2+M(A-f')=0 \tag{3.31}$$

$$\theta''+Prf\theta'+PrNb\phi'\theta'+PrNt(\theta')^2=0 \tag{3.32}$$

$$\phi''+Le\,Pr\,f\,\phi'+\frac{Nt}{Nb}\theta''=0. \tag{3.33}$$

The dimensionless conditions associated with the boundary are as follows:

$$\left.\begin{aligned}
&f(0)=0,\\
&f'(0)=1+\delta\left(1+\frac{1}{\gamma}\right)f''(0),\\
&\theta'(0)=-B_i[1-\theta(0)], \qquad \phi(0)=1, \quad \text{at} \quad \eta=0,\\
&f'(\infty)\to A, \qquad \theta(\infty)\to 0, \qquad \phi(\infty)\to 0, \quad as \quad \eta\to\infty
\end{aligned}\right\} \tag{3.34}$$

The following expression refers to different parameters used in the above equations:

$$\left.\begin{aligned}
A&=\frac{b}{a},\\
Pr&=\frac{\nu}{\alpha},\\
\delta&=\mu_\beta\sqrt{\frac{a}{\nu}}\\
Le&=\frac{\alpha}{D_B} \qquad ,\\
M&=\frac{\sigma B_0^2}{\rho_f a},\\
Bi&=\frac{h_f}{k}\sqrt{\frac{\nu}{a}},\\
Nb&=\frac{(\rho C)_p}{(\rho C)_f\nu}D_B(C_w-C_\infty),\\
Nt&=\frac{(\rho C)_p}{(\rho C)_f\nu}D_T(T_w-T_\infty)
\end{aligned}\right\} \tag{3.35}$$

The coefficient of skin friction, is as follows:

$$C_f=\frac{\tau_w}{\rho u_w^2} \tag{3.36}$$

where

$$\begin{aligned}\tau_w &= \left(\mu_B + \frac{P_y}{\sqrt{2\pi_c}}\right)\left(\frac{\partial u}{\partial y}\right),\\ &= \mu\big(1 + \frac{P_y}{\mu\sqrt{2\pi_c}}\right)\left(\frac{\partial u}{\partial y}\right),\\ &= \tau\mu_B\left(1+\frac{1}{\gamma}\right)\frac{\partial u}{\partial y}, \end{aligned} \tag{3.37}$$

$$u_w(x) = ax, \tag{3.38}$$

$$\begin{aligned}\frac{\partial u}{\partial y} &= axf''\sqrt{\frac{a}{\nu}},\\ &= a\sqrt{\frac{a}{\nu}}xf'', \end{aligned} \tag{3.39}$$

Using (3.37)-(3.39) in (3.36), we get

$$\begin{aligned}C_f &= \frac{\mu_B\left(1+\frac{1}{\gamma}\right)a\sqrt{\frac{a}{\nu}}xf''}{\rho a^2x^2},\\ &= \frac{\frac{\nu}{\sqrt{\nu}}\left(1+\frac{1}{\gamma}\right)a\sqrt{a}xf''}{a^2x^2},\\ &= \frac{\frac{\nu}{\sqrt{\nu}}\left(1+\frac{1}{\gamma}\right)a\sqrt{a}xf''}{ax},\\ &= \frac{\sqrt{\nu}}{\sqrt{a}x}\left(1+\frac{1}{\gamma}\right)f'', \end{aligned} \tag{3.40}$$

$$\begin{aligned}C_f\left(\frac{\sqrt{a}x}{\sqrt{\nu}}\right) &= \left(1+\frac{1}{\gamma}\right)f'',\\ C_f\frac{\sqrt{a}}{\sqrt{\nu}}\sqrt{x}\sqrt{x} &= \left(1+\frac{1}{\gamma}\right)f'',\\ C_f\frac{\sqrt{ax}}{\sqrt{\nu}}\sqrt{x} &= \left(1+\frac{1}{\gamma}\right)f'',\\ C_f\frac{\sqrt{u_w}\sqrt{x}}{\sqrt{\nu}} &= \left(1+\frac{1}{\gamma}\right)f''. \end{aligned} \tag{3.41}$$

As

$$Re_x = \frac{U_w.x}{\nu}, \tag{3.42}$$

so

$$\begin{aligned} Re_x^{\frac{1}{2}} &= \frac{U_w^{\frac{1}{2}}.x^{\frac{1}{2}}}{\nu^{\frac{1}{2}}} \\ &= \frac{\sqrt{u_w}\sqrt{x}}{\sqrt{\nu}} \\ C_f Re_x^{\frac{1}{2}} &= \left(1+\frac{1}{\gamma}\right) f''. \end{aligned} \tag{3.43}$$

The local Nusselt number is characterized as:

$$Nu_x = \frac{xq_w}{k(T_w - T_\infty)},$$

where

$$q_w = -k\left(\frac{\partial T}{\partial y}\right)_{y=0},$$

and

$$\frac{\partial T}{\partial y} = \sqrt{\frac{a}{\nu}}\Big(T_w - T_\infty\Big)\theta'(0)$$

Using (3.44) in (3.44) and (3.44) in (3.44)

$$\begin{aligned} Nu_x &= -x\sqrt{\frac{a}{\nu}} \quad \theta'(0) \\ \Rightarrow \quad Nu_x &= -\frac{\sqrt{x}\sqrt{x}\sqrt{a}}{\theta}{}'\sqrt{\nu} \\ \Rightarrow \quad Nu_x &= -\frac{\sqrt{x}\sqrt{ax}}{\theta}{}'\sqrt{\nu} \end{aligned}$$

$$\Rightarrow \quad \frac{Nu_x}{\sqrt{Rex}} = -\theta'(0). \tag{3.44}$$

The local Sherwood number is characterized as:

$$Shx = \frac{xhm}{D_B}(C_w - C_\infty),$$

where

$$hm = -D_B\left(\frac{\partial \phi}{\partial y}\right)$$

Now

$$\begin{aligned} \phi &= (C_w - C_\infty)\phi + C_\infty \\ \Rightarrow \quad \frac{\partial \phi}{\partial y} &= \sqrt{\frac{a}{\nu}}(C_w - C_\infty)\phi' \end{aligned} \tag{3.45}$$

Using (3.45) in (3.45),

$$hm = -D_B\sqrt{\frac{a}{\nu}}(C_w - C_\infty)\phi'(0) \tag{3.46}$$

Using (3.46) in (3.45),

$$\begin{aligned} Shx &= -\frac{xDB\sqrt{\frac{a}{\nu}}(C_w - C_\infty)\phi'(0)}{DB(C_w - C_\infty)} \\ &= -x\sqrt{\frac{a}{\nu}} \qquad \phi'(0) \\ &= \frac{-\sqrt{x}\sqrt{ax}\phi^{(0)}}{\sqrt{\nu}} \\ &= -\sqrt{Rx} \quad \phi'(0) \\ \Rightarrow \quad \frac{Shx}{\sqrt{Rx}} &= -\phi'(0). \end{aligned} \tag{3.47}$$

3.3 Solution Approach

In order to solve the system of ODEs (3.30) - (3.32) subject to the boundary conditions (3.5), the shooting technique has been used. Basically, equation (3.30) is solved numerically and afterward the computed results of f, f' and f'' are used in equations (3.31)-(3.32). For the numerical treatment of equation (3.30), the missing initial condition $f''(0)$ has been denoted as p and the following notations

have been considered.

$$\begin{aligned} f &= g_1, \\ f' &= g_1' = g_2, \\ f'' &= g_1'' = g_2' = g_3, \\ \frac{\partial f}{\partial p} &= g_4, \\ \frac{\partial f'}{\partial p} &= g_5, \\ \frac{\partial f''}{\partial p} &= g_6, \end{aligned} \tag{3.48}$$

The equation (3.30) can be translated into a scheme of three first-order ODEs using the upward notations. The reduced form of (3.30) is the first three of the ODEs and the remaining three are obtained by differentiating the first three w.r.t p.

$$\begin{aligned} g_1^{'} &= g_2; & g_1(0) &= 0 \\ g_2^{'} &= g_3; & g_2(0) &= 1 + \delta\left(1 + \frac{1}{\gamma}\right)g \\ g_3^{'} &= \frac{\gamma}{\gamma+1}\Big[-g_1 g_3 + g_2^2 - A^2 - M(A - g_2)\Big]; & g_3(0) &= p \\ g_4^{'} &= g_5; & g_4(0) &= 0 \\ g_5^{'} &= g_6; & g_5(0) &= \delta\left(1 + \frac{1}{\gamma}\right) \\ g_6^{'} &= \frac{\gamma}{\gamma+1}\Big[-g_4 g_3 - g_1 g_6 + 2g_2 g_5 + M g_5\Big]; & g_6(0) &= 1 \end{aligned} \tag{3.49}$$

The RK-4 technique has been used to tackle the above initial value problem. In order to get the approximate numerical results, the problem's domain is considered to be bounded i.e $[0, \eta_\infty]$, where η_∞ is chosen to be an appropriate finite positive real number so that the variation in the result for $\eta \succcurlyeq \eta_\infty$ is ignorable. The missing condition for the above system of equations is to be picked to such an extent that

$(g_2(\infty))_p = A$. This mathematical equation was solved using the method of the Newton defined by the following iterative scheme.

$$p^{(n+1)} = p^{(n)} - \frac{(g_2(\eta_\infty))_{g=g^{(n)}} - A}{\left(\frac{\partial g_2(\eta_\infty)}{\partial g}\right)_{p=p^{(n)}}}, \tag{3.50}$$

$$p^{(n)} - \frac{(g_2(\eta_\infty))_{p=p^{(n)}} - A}{(g_2(\eta_\infty))_{p=p^{(n)}}}, \tag{3.51}$$

The stoping criteria for the shooting strategy is set as,

$$|(g_2(\eta_\infty)) - A| \lessdot \epsilon, \tag{3.52}$$

for some sufficiently small positive number ϵ,

Now to solve the equations (3.31) and (3.32) numerically, the missing initial conditions $\theta(0)$ and $\phi(0)$ have been denoted by s and t, respectively. The following notations were therefore taken into consideration.

$$\left.\begin{array}{llllll} \theta = y_1,\ \theta^{'} = y_2,\ \phi = y_3, & \phi^{'} = y_4, & \dfrac{\partial\theta}{\partial s} = y_5, & \dfrac{\partial\theta^{'}}{\partial s} = y_6, & \dfrac{\partial\phi}{\partial s} = y_7, \\ \dfrac{\partial\phi^{'}}{\partial s} = y_8, & \dfrac{\partial\theta}{\partial t} = y_9, & \dfrac{\partial\theta^{'}}{\partial s} = y_{10}, & \dfrac{\partial\phi}{\partial s} = y_{11}, & \dfrac{\partial\phi^{'}}{\partial t} = y_{12}. \end{array}\right\} \tag{3.53}$$

Joining the above notations, a system of first order ODEs is accomplished that is expressed below.

$$\begin{aligned}
y_1' &= y_2, & y_1(0) &= s, \\
y_2' &= -PrCy_2 - PrNby_4y_2 - PrNty_2^2, & y_2(0) &= -Bi[1-s], \\
y_3' &= y_4, & y_3(0) &= 1, \\
y_4' &= -LePrCy_4 + \frac{Nt}{Nb}\left[+PrCy_2 + PrNby_4y_2 + PrNty_2^2\right], & y_4(0) &= t, \\
y_5' &= y_6, & y_5(0) &= 1, \\
y_6' &= -PrCy_6 - PrNb(y_4y_6 + y_2y_8) - 2PrNty_2y_6, & y_6(0) &= Bi,
\end{aligned}$$

$$
\begin{aligned}
y_7' &= y_8, && y_7(0) = 0,\\
y_8' &= -LePrCy_8 + \frac{Nt}{Nb}\Big[PrCy_6 + PrNb(y_8y_2 + y_4y_6)\\
&\quad + 2PrNty_2y_6\Big], && y_8(0) = 0,\\
y_9' &= y_{10}, && y_9(0) = 0,\\
y_{10}' &= -PrCy_{10} - PrNb(y_{12}y_2 + y_4y_{10}) - 2PrNty_2y_{10}, && y_{10}(0) = 0,\\
y_{11}' &= y_{12}, && y_{11}(0) = 0,\\
y_{12}' &= -LePrCy_{12} + \frac{Nt}{Nb}\Big[prCy_{10} + PrNb(y_{12}y_2 + y_4y_{10})\\
&\quad + 2PrNty_2yy_{10}\Big], && y_{12}(0) = 1.
\end{aligned}
$$

The RK-4 technique has been taken into consideration for tackling the above initial value problem. For the above system of equations, the missing conditions s and t are to be specify such that:

$$
(y_1(s,t))\eta = \eta_\infty = 0, \qquad (y_3(s,t))\eta = \eta_\infty = 0 \tag{3.54}
$$

The above algebraic equations have been solved by utilizing the Newton's strategy represented by the ensuring iterative formula.

$$
\begin{aligned}
\begin{bmatrix} s^{(n+1)} \\ t^{(n+1)} \end{bmatrix} &= \begin{bmatrix} s^{(n)} \\ t^{(n)} \end{bmatrix} - \left[\begin{bmatrix} \frac{\partial y_1(s,t)}{\partial s} & \frac{\partial y_3(s,t)}{\partial s} \\ \frac{\partial y_1(s,t)}{\partial t} & \frac{\partial y_3(s,t)}{\partial t} \end{bmatrix}^{-1} \begin{bmatrix} y_1 \\ y_2 \end{bmatrix} \right]_{\left(s^{(n)}, t^{(n)}, \eta_\infty\right)}\\
\Rightarrow \begin{bmatrix} s^{(n+1)} \\ t^{(n+1)} \end{bmatrix} &= \begin{bmatrix} s^{(n)} \\ t^{(n)} \end{bmatrix} - \left[\begin{bmatrix} y_5 & y_9 \\ y_7 & y_{11} \end{bmatrix}^{-1} \begin{bmatrix} y_1 \\ y_2 \end{bmatrix} \right]_{\left(s^{(n)}, t^{(n)}, \eta_\infty\right)}
\end{aligned} \tag{3.55}
$$

The stoping criteria for the shooting technique is set as:

$$
max\{|\,(y_1(\xi\infty)\,|,\ |\,(y_3(\xi\infty))\,|\} < \epsilon,
$$

for some exceptionally small positive number ϵ. All through this chapter, ϵ has been taken as 10^{-12} while η_∞ is set as 7.

3.4 Analysis of Results

This section addresses the numerical solutions in detail, using graphs and tables. This will primarily address the velocity, temperature, and concentration profile. The present results will be compared with those of [25] for verification of the code. The numerical calculations are executed for the observation of the impact of relevant physical parameters like, Casson fluid parameter γ, slip parameter δ, velocity correlation parameter A, Biot number Bi, Brownian motion parameter Nb, thermophoresis parameter Nt, Lewis number Le on the skin friction coefficient, Nusselt number, and Sherwood number. Such related physical parameters have an immediate effect on distributions of velocity , temperature and concentration. Table 3.1 shows the numerical results of the skin-friction coefficient along with the Nusselt and sherwood numbers for the current model in respect of a shift in the values of various parameters such as A, δ, γ, Nb, Nt, Pr, Le, Bi and M. From the results, it was noted that the skin-friction coefficient decreases for the larger values of A and δ, while heat and mass transfer rates increase significantly.
Table 3.2 portray the intervals I_f, I_θ and I_ϕ where from the missing initial conditions $f''(0)$, $\theta'(0)$ and $\phi'(0)$ respectively can be chosen. It is noteworthy that the intervals mentioned offer a considerable flexibility for the choice of initial guesses.

3.4.1 Influence of Casson Parameter on The Skin Friction

Figure 3.2 is drawn to investigate the effect of γ on the velocity filed. The fluid velocity increases with an increasing values of γ. Physically, the consistency of the fluid increment due to the escalation of the γ values and then decreases, the fluid's velocity profile also decreases the velocity boundary layer thickness for uprising

values of γ. Furthermore, the present phenomenon change to Newtonian fluid when γ tends to infinity.

3.4.2 Impact of Slip Parameter on The Skin Friction

Figure 3.3 indicates the impact of δ on the distribution of dimensionless velocity. It is clearly shown that by an an enhancing values of δ the velocity profile arises. Generally, the growing values of δ create a frictional resistance between the surface of the sheet and fluid particles escalates, which causes a decrement of the fluid velocity.

3.4.3 Impact of Velocity Ratio on Skin Friction Parameter

Figure 3.4 analyzes the effect of A on the distribution of dimensionless velocity. From the figure it is apparent that when the free stream velocity is greater than the surface velocity, while the fluid particle velocity accelerates at $A > 1$. In addition the thickness of the boundary layer decelerates by increasing the A values. In fact, if the stretching velocity is less than the free-stream velocity the velocity graph tends to be A. Often, when the extending sheet velocity is greater than the free-stream velocity, which creates a fluid velocity declaration.

3.4.4 Biot Number Impact on Temperature Profile

Figure 3.5 reflects the influence of Bi on the dimensionless temperature distribution. The graph of the velocity profile specify that an increment in Bi causes an enhancement in the temperature profile. Generally, Biot number is expressed as the ratio of temperature change at the surface to conduction within the surface of the body. As expected, the boosting values of Bi enhanced the thermal boundary layer of the fluid.

3.4.5 Influence of Brownian Motion Parameter on Profile Temperature

Figure 3.6 analyzes the impact of Nb on the temperature profile. The temperature distribution enhances with the uprising values of Nb. It is observed that a higher Nb intensifies the fluid temperature owing to more collision between the fluid particles.

3.4.6 Impact of Thermophoresis Parameter on The Temperature Profile

Figure 3.7 illustrates the Nt effect on temperature distribution. From the figure it is transparent that the θ field is improved for moderately enlarging values of Nt. In addition, the particles Nt apply a force on the other particles because of which these particles shift from the hotter to less region. Therefore, there is an intensification of the fluid's θ profile.

3.4.7 Impact of Slip Parameter on The Temperature Profile

Figure 3.8 illustrates the influence of δ on temperature distribution, from the figure it is apparent that especially for cautiously enlarging values of δ, the temperature field is enhanced. Increasing the values of δ actually the thermal boundary layer depth also raises the sheet surface temperature.

3.4.8 Effect of Velocity Ratio on The Temperature Profile

Figure 3.9 displays the effect of A on temperature distribution. We note that for boosting A values, the temperature distribution decreases. In addition, the depth of the thermal boundary layer decreases as the values of A increase.

3.4.9 Impact of Casson Parameter on The Temperature Profile

Figure 3.10 reveals the impact of γ on temperature distribution. The escalating values of γ by which the mounting values of temperature depiction. Generally the thermal boundary layer depth uprise by increasing values of γ due to which the surface temperature enlarge with γ.

3.4.10 Impact of Lewis Number on Profile of Concentration

Figure 3.11 shows the connection between Lewis numbers and the dimensional concentration distribution. Concentration profile decelerates for the boosting values of Le and therefore we have get a small molecular diffusivity and thermal boundary layer.

3.4.11 Impact of Biot Number on Profile of Concentration

Figure 3.12 manifests the relationship between Bi and the concentration profile. For boosting values of Bi the graph of dimensionless concentration profile is increased. Increasing Bi means a decrement in the fluid's conductivity as a result of which the boundary layer of concentration is increased.

3.4.12 Impact of Thermophoresis Parameter on Profile of Concentration

Figure 3.13 illustrates the impact of Nt on both temperature and concentration distribution, from the figure it is clear that for gradually enlarging values of Nt both the temperature and concentration field is enhanced.

3.4.13 Impact of Casson Parameter on The Skin Friction

Figure 3.14 shows the relationship between γ and the concentration profile. Moreover, the concentration of fluid and its associative boundary thickness are enlarges by mounting values of γ. Figures [3.15]-[3.17] are sketched to demonstrate the effect of skin friction coefficient against magnetic parameter to increase values of Casson parameter, slip parameter and velocity ratio parameter.

3.4.14 Impact of Casson Parameter on The Skin Friction

It is noted in Figure 3.15 that with an increment in the Casson fluid parameter the skin friction coefficient decreases significantly, which implies that the drag forces on the surface reduces effectively.

3.4.15 Effect on Skin Friction by Slip Parameter

Figure 3.16 reflect that the skin friction coefficient increases effectively with increased slip parameter.

3.4.16 Effect of Parameter Velocity Ratio on Skin Friction

Figure 3.17 displays that with an enhancement in velocity ratio parameter, the skin friction coefficient reduces effectively.

3.4.17 Impact of The Nusselt Number on The Brownian Motion Parameter

Figure 3.18 portrays the impact of Nb on Nu_x plotted against Nt. As the estimations of the two parameters Nt and Nb increases, the nearby Nu_x decreases.

3.4.18 Lewis Number Effect on The Sherwood Number

Figure 3.19 displays the impact of Le on Sh_x as for Biot number. It is seen that local Sherwood number increases with an increase in the Lewis number. It can be noted that,the field Nu_x is also increased by enhancing the values of Le whenever the N_ux expands; as the estimations of Bi as well increases the nearby Sh_x decreases.

TABLE 3.1: "Numerical results of the coefficient of skin friction , Nusselt, and Sherwood numbers".

A	δ	γ	N_b	N_t	P_r	L_e	B_i	M	$-f''(0)$	$-\theta'(0)$	$-\phi'(0)$
0.0	0.1	10	0.1	0.1	10	10	0.1	1.0	1.1415	0.0894	7.2259
0.1	—	—	—	—	—	—	—	—	1.0653	0.0896	7.2857
0.2	—	—	—	—	—	—	—	—	0.9792	0.0898	7.3519
0.3	—	—	—	—	—	—	—	—	0.8838	0.0900	7.4237
0.9	—	—	—	—	—	—	—	—	0.1467	0.0911	7.9377
1.5	—	—	—	—	—	—	—	—	-0.8188	0.0920	8.5325
2.0	—	—	—	—	—	—	—	—	-1.7623	0.0926	9.0553
2.4	—	—	—	—	—	—	—	—	-2.5944	0.0930	9.4812
0.4	0.2	—	—	—	—	—	—	—	0.6758	0.0899	7.2452
—	0.4	—	—	—	—	—	—	—	0.5357	0.0894	6.8775
—	0.6	—	—	—	—	—	—	—	0.4449	0.0891	6.6223
—	0.8	—	—	—	—	—	—	—	0.3810	0.0888	6.4333
—	0.4	0.1	—	—	—	—	—	—	0.0908	0.0887	6.2009
—	—	0.5	—	—	—	—	—	—	0.2563	0.0892	6.6086
—	—	1	—	—	—	—	—	—	0.3477	0.0893	6.7254
—	—	10	—	—	—	—	—	—	0.5357	0.0894	6.8776
—	—	10	—	—	—	—	—	—	0.5688	0.0894	6.8968

TABLE 3.2: "The intervals for the initial guesses for the missing initial conditions".

A	δ	γ	Nb	Nt	Pr	Le	Bi	M	I_f	I_θ	I_ϕ
0.0	0.1	10	0.1	0.1	10	10	0.1	1	[-1.0,-0.9]	[-1.1,20.4]	[-1.1,30.7]
0.1	—	—	0.1	0.1	10	10	0.1	1	[-0.9,-0.5]	[-1.0,30.5]	[-1,40.7]
0.2	—	—	—	—	—	—	—	—	[-1.0,-0.3]	[-1.0,30.6]	[-1.0,40.5]
0.3	—	—	—	—	—	—	—	—	[-0.9,0.2]	[-0.9,1.8]	[-0.9,0.9]
0.9	—	—	—	—	—	—	—	—	[-0.1,1.2]	[-0.1,1.5]	[-0.1,1.6]
1.5	—	—	—	—	—	—	—	—	[1.0,1.5]	[1.0,1.9]	[1.0,2.5]
2.0	—	—	—	—	—	—	—	—	[1.7,2.8]	[1.7,10.9]	[1.7,9.9]
2.4	—	—	—	—	—	—	—	—	[2.5,3.6]	[-0.5,195.5]	[-0.5,20.5]
0.4	0.2	—	—	—	—	—	—	—	[-0.7,0.4]	[-0.9,99.5]	[-0.9,88.2]
—	0.4	—	—	—	—	—	—	—	[-0.5,0.3]	[-0.9,85.0]	[-0.9,72.5]
—	0.6	—	—	—	—	—	—	—	[-0.4,0.2]	[-0.5,110.0]	[-0.5,130.0]
—	0.8	—	—	—	—	—	—	—	[-0.5,0.3]	[-0.7,210.1]	[-0.7,215.0]
—	0.4	0.1	—	—	—	—	—	—	[-0.3,3.2]	[-0.9,45.5]	[-0.9,80.0]
—	—	0.5	—	—	—	—	—	—	[-0.4,0.2]	[-0.9,85.0]	[-0.9,80.0]
—	—	1	—	—	—	—	—	—	[-0.3,1.3]	[-2.5,70.0]	[-2.5,85.0]
—	—	10	—	—	—	—	—	—	[-0.5,0.3]	[-2.5,70.0]	[-2.5,85.0]
—	—	10	—	—	—	—	—	—	[-0.6,0.2]	[-3.5,80.9]	[-3.5,89.1]

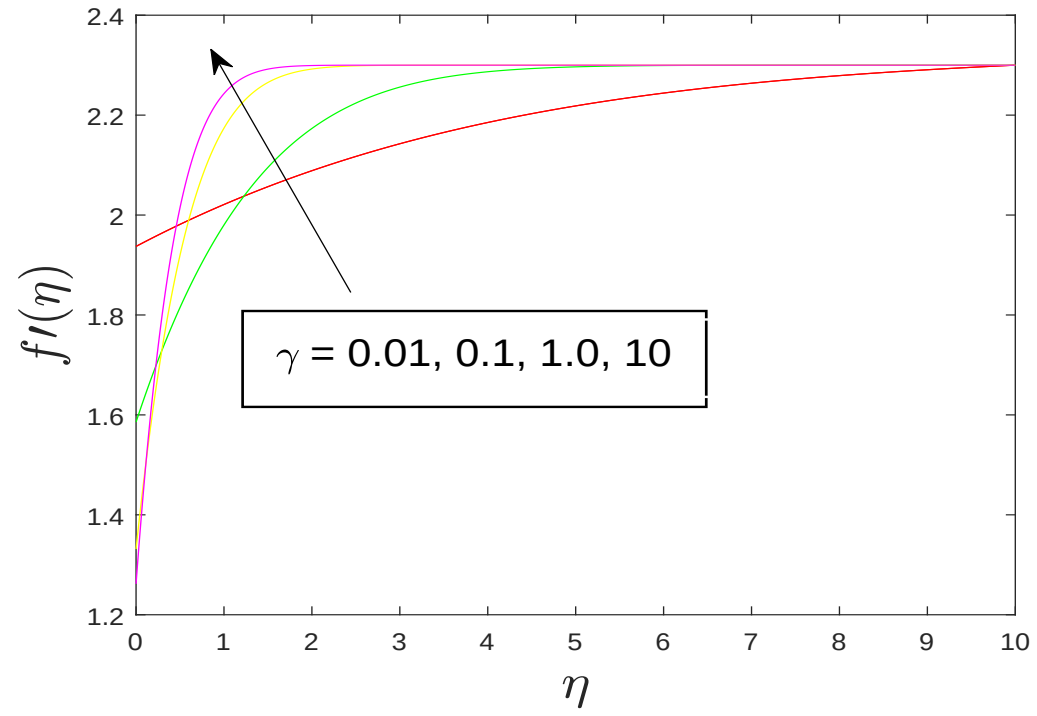

FIGURE 3.2: "Influence of γ on $f'(\eta)$ when $\delta = 0.1$, $A = 2.3$, $M = 1$"

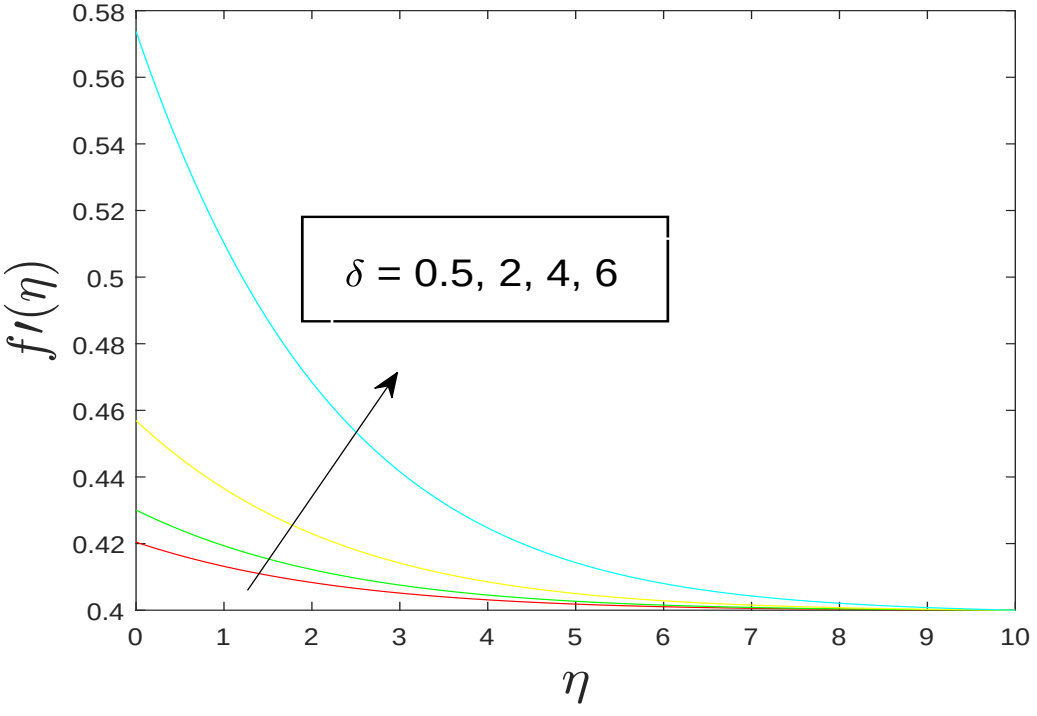

FIGURE 3.3: "Influence of δ on $f'(\eta)$ when $\gamma = 0.1$, $A = 0.4$, $M = 1$"

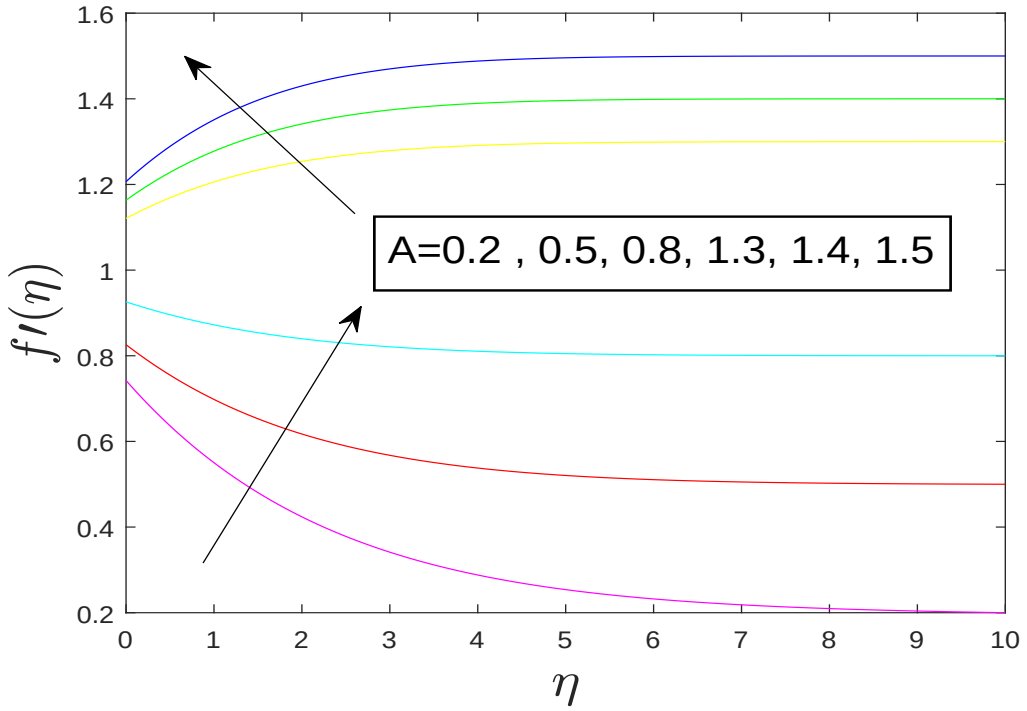

FIGURE 3.4: "Impact of A on $f'(\eta)$ when $\gamma = 0.1$, $\delta = 0.1$, $M = 1$"

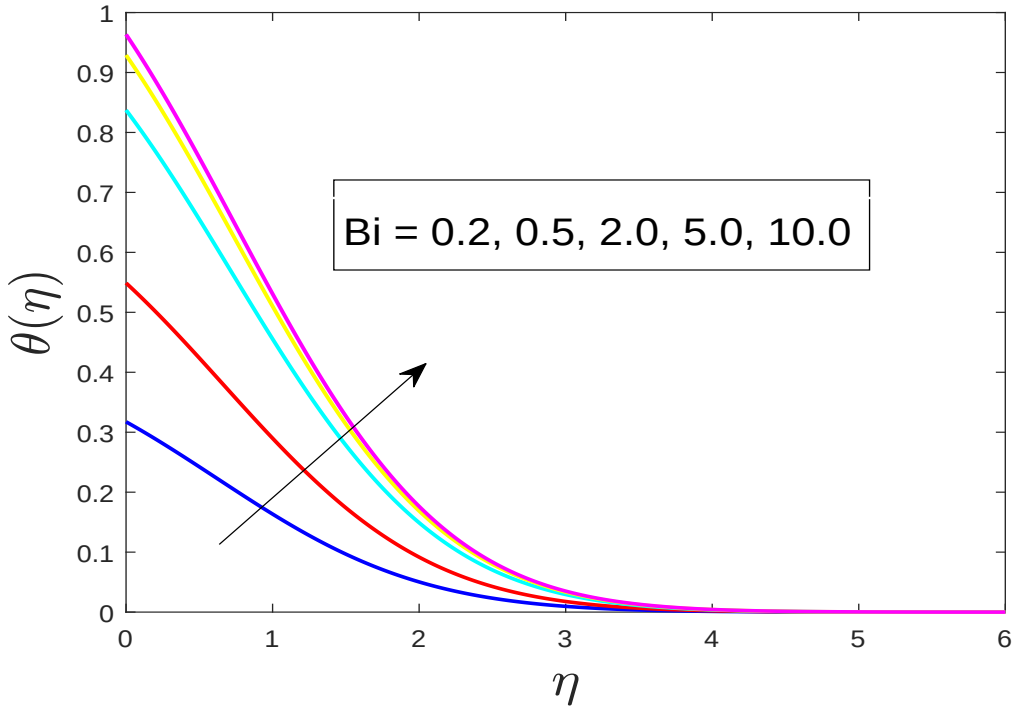

FIGURE 3.5: "Influence of Bi on $\theta(\eta)$ when $Nb = Nt = 0.5$, $Le = 2$, $\gamma = 0.1$, $\delta = 0.2$, $Pr = M = 1$, $A = 0.4$"

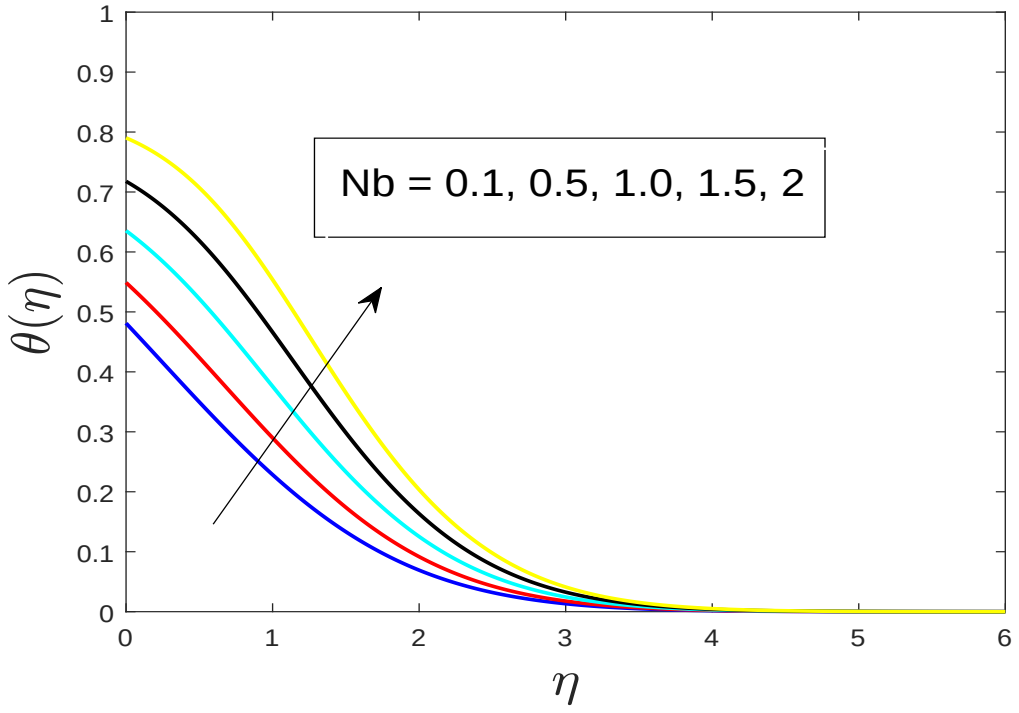

FIGURE 3.6: "Influence of Nb on $\theta(\eta)$ when $Nt = 0.5$, $Le = 2$, $\gamma = 0.1$, $\delta = 0.2$, $Pr = M = 1$, $A = 0.4$"

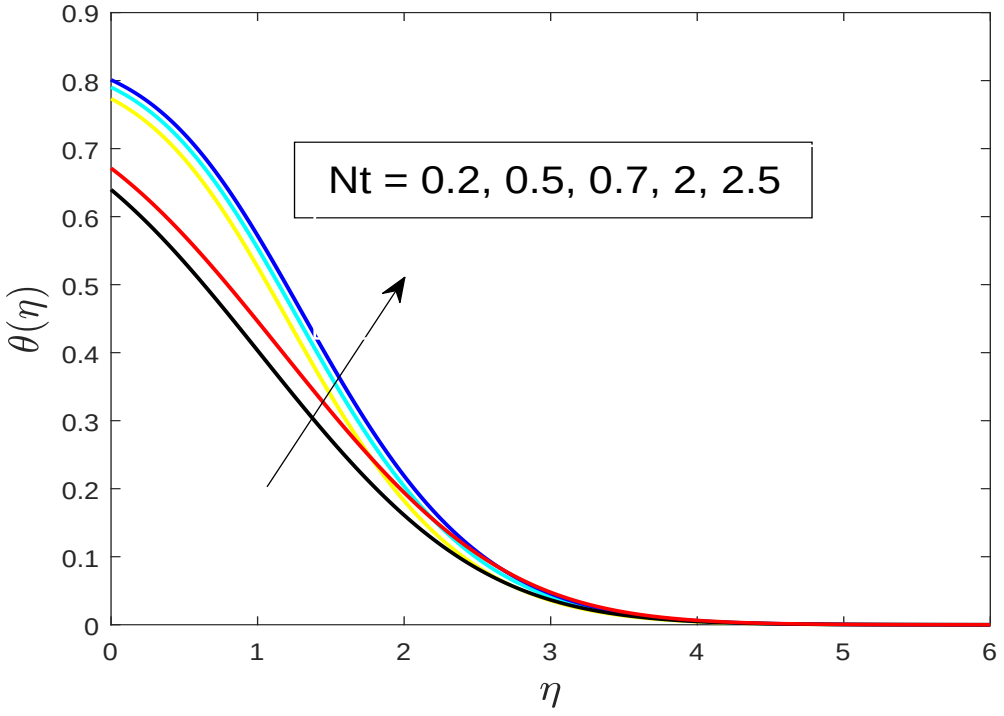

FIGURE 3.7: "Influence of Nt on $\theta(\eta)$ when $Nb = 0.5$, $Le = 2$, $\gamma = 0.1$, $Bi = 0.5$, $\delta = 0.2$, $Pr = M = 1$, $A = 0.4$"

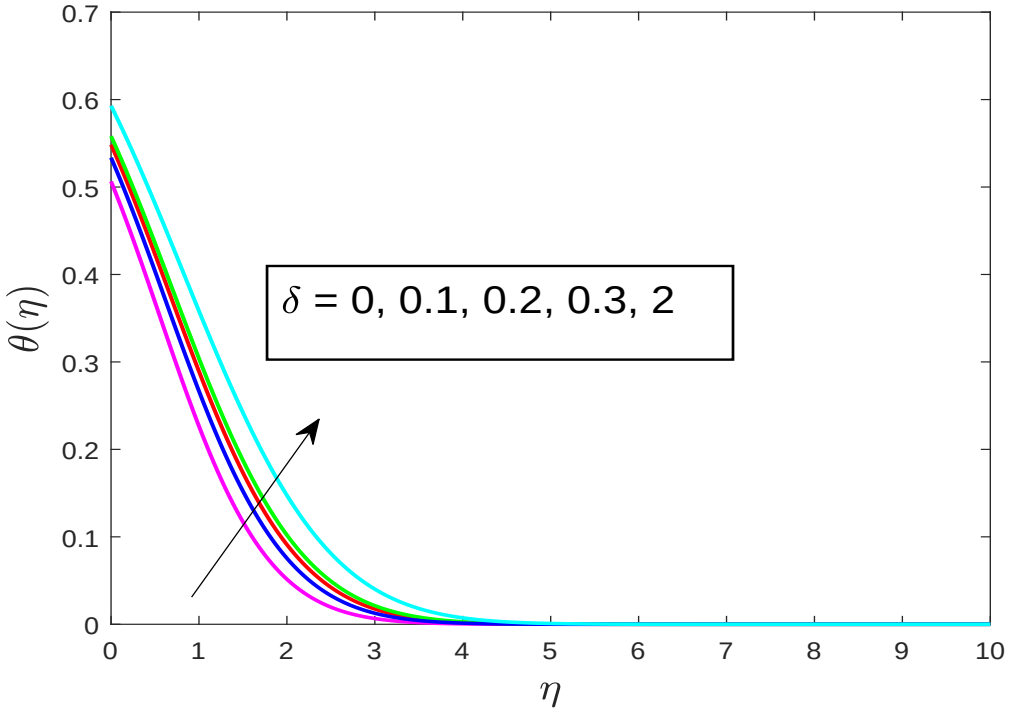

FIGURE 3.8: "Impact of δ on $\theta(\eta)$ when $Nb = Nt = 0.5$, $Le = 2$, $\gamma = 0.1$, $Bi = 0.5$, $Pr = M = 1$, $A = 0.4$"

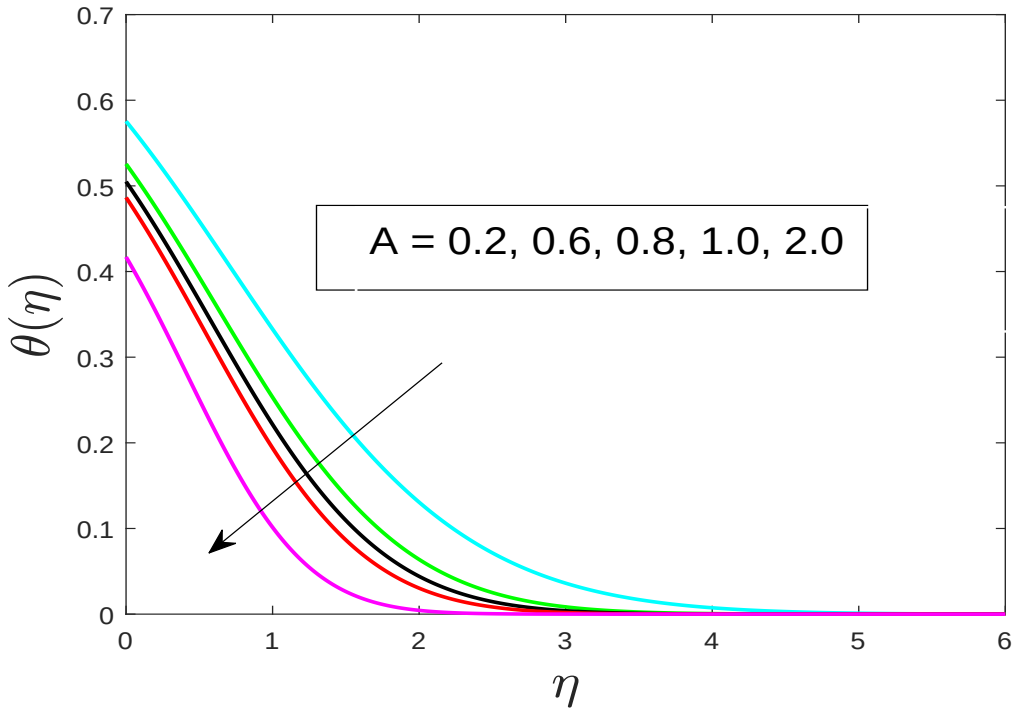

FIGURE 3.9: "Influence of A on $\theta(\eta)$ when $Nb = Nt = 0.5$, $Le = 2$, $\gamma = 0.1$, $Bi = 0.5$, $Pr = M = 1$, $Bi = 0.5$, $\delta = 0.2$"

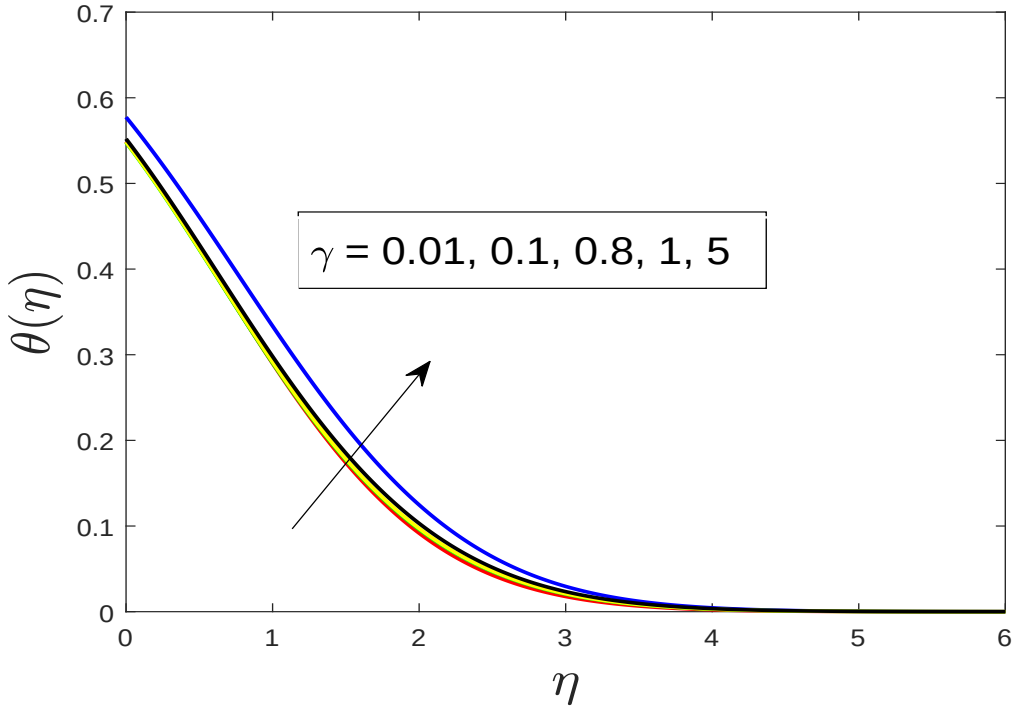

FIGURE 3.10: "Influence of γ on $\theta(\eta)$ when $Nb = Nt = 0.5$, $Le = 2$, $A = 0.4$, $Bi = 0.5$, $Pr = M = 1$, $\delta = 0.2$"

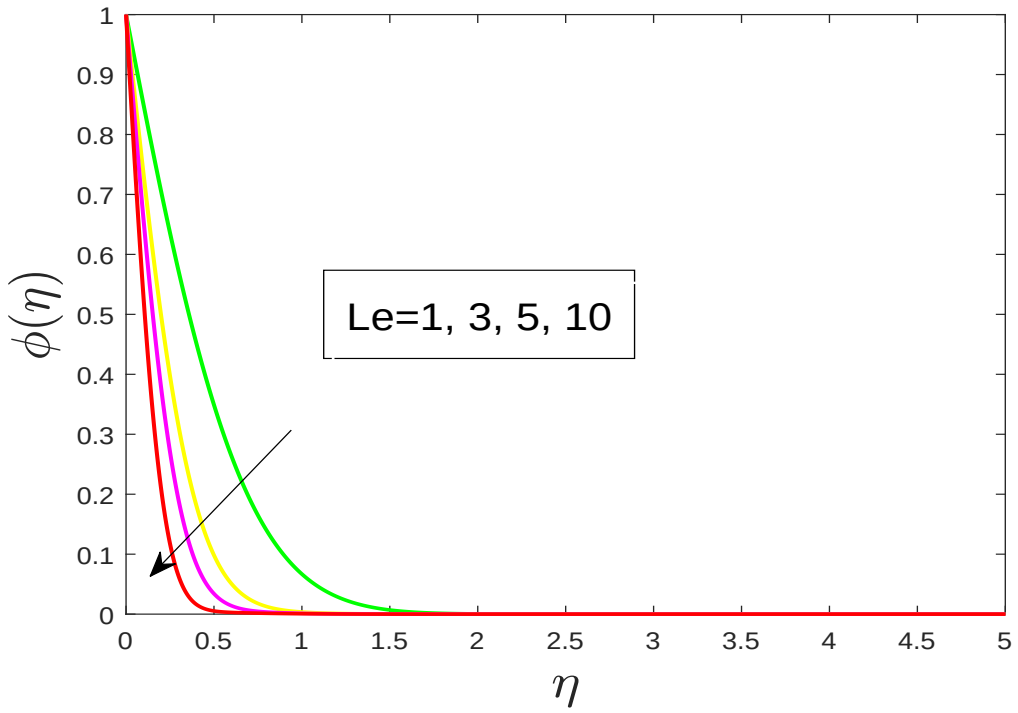

FIGURE 3.11: "Impact of Le on $\phi(\eta)$ when $Nb = Nt = Bi = 0.1$, $Pr = 5$, $A = 0.4$, $Bi = 0.5$, $M = 1$, $\delta = 0.1$, $\gamma = 0.2$"

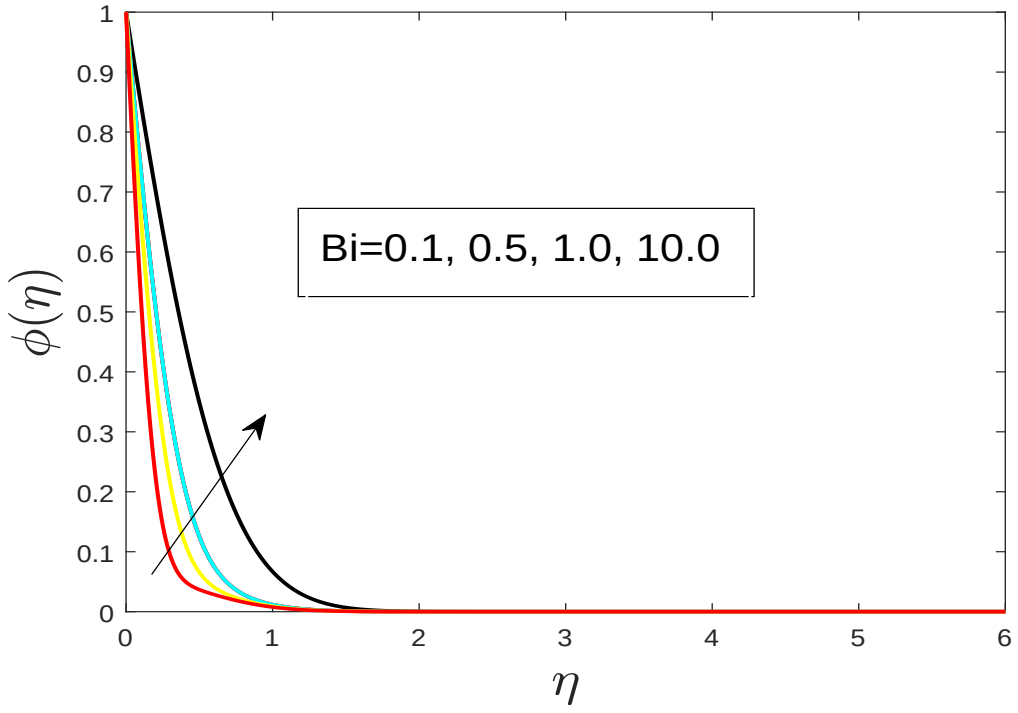

FIGURE 3.12: "Influence of Bi on $\phi(\eta)$ when $Nb = Nt = 0.1$, $Pr = 5$, $A = 0.4$, $M = 1$, $\delta = 0.1$, $\gamma = 0.2$"

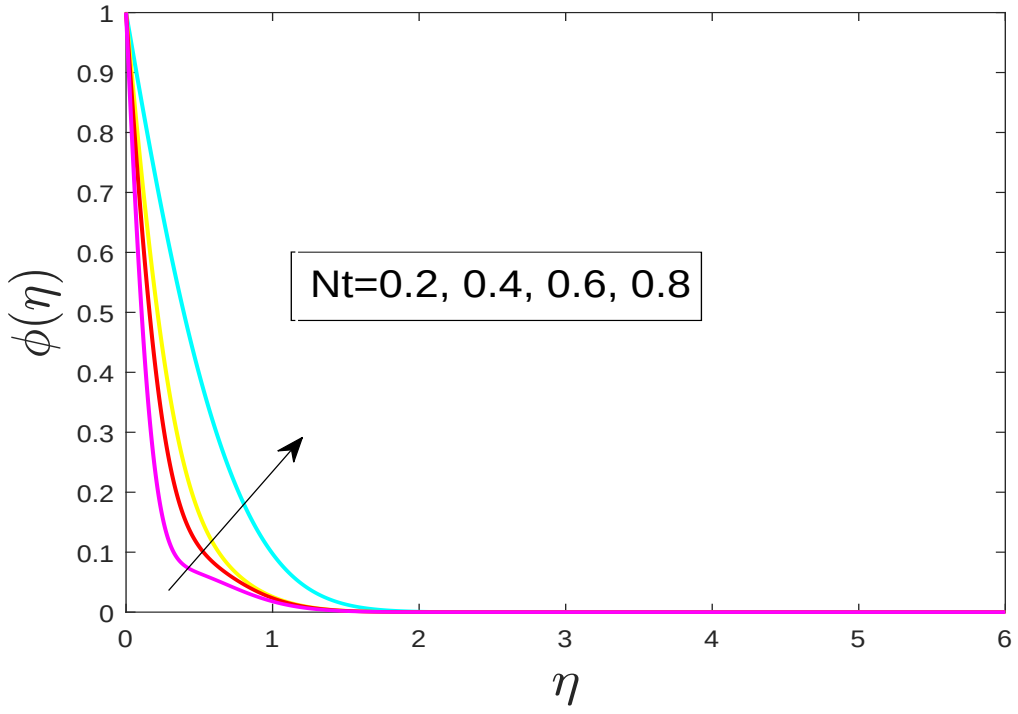

FIGURE 3.13: "Impact of Nt on $\phi(\eta)$ when $Nb = 0.1$, $Pr = 5$, $A = 0.4$, $M = 1$, $\delta = 0.1$, $Bi = \gamma = 0.2$"

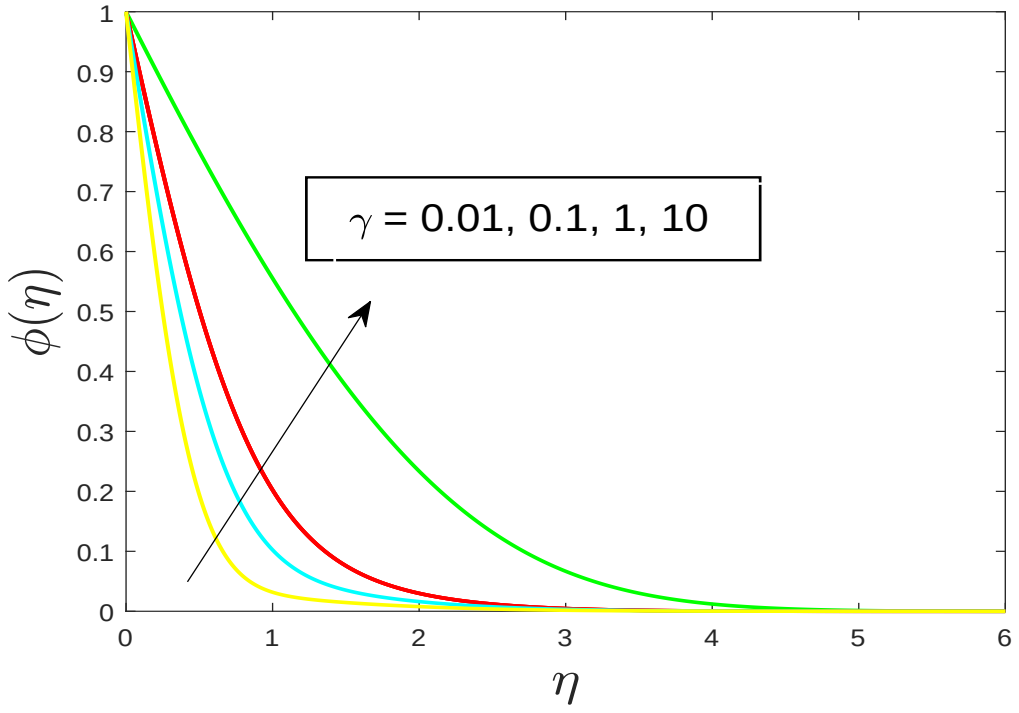

FIGURE 3.14: "Influence of γ on $\phi(\eta)$ when $Nb = Nt = 0.2$, $Pr = M = 1$, $A = 0.4$, $M = 1$, $\delta = 0.1$, $Bi = 0.5$, $A = 0.4$"

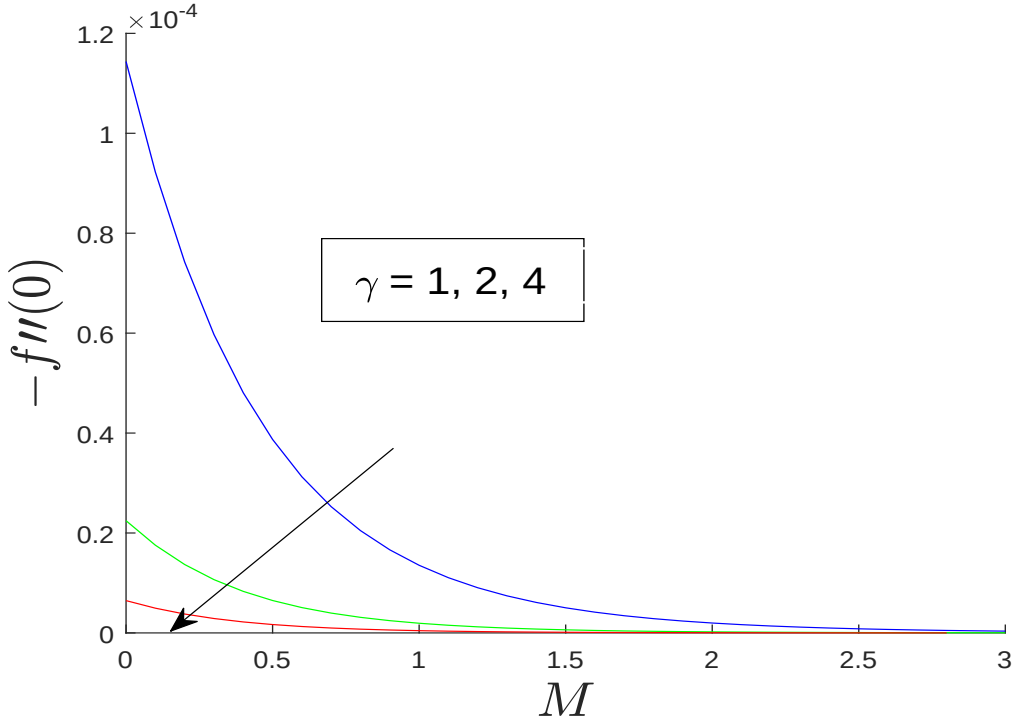

FIGURE 3.15: "Impact of γ on $-f''(0)$ when $Nb = Nt = 0.1$, $Pr = 2$, $A = 0.1$, $Bi = 10$, $\delta = 0.2$"

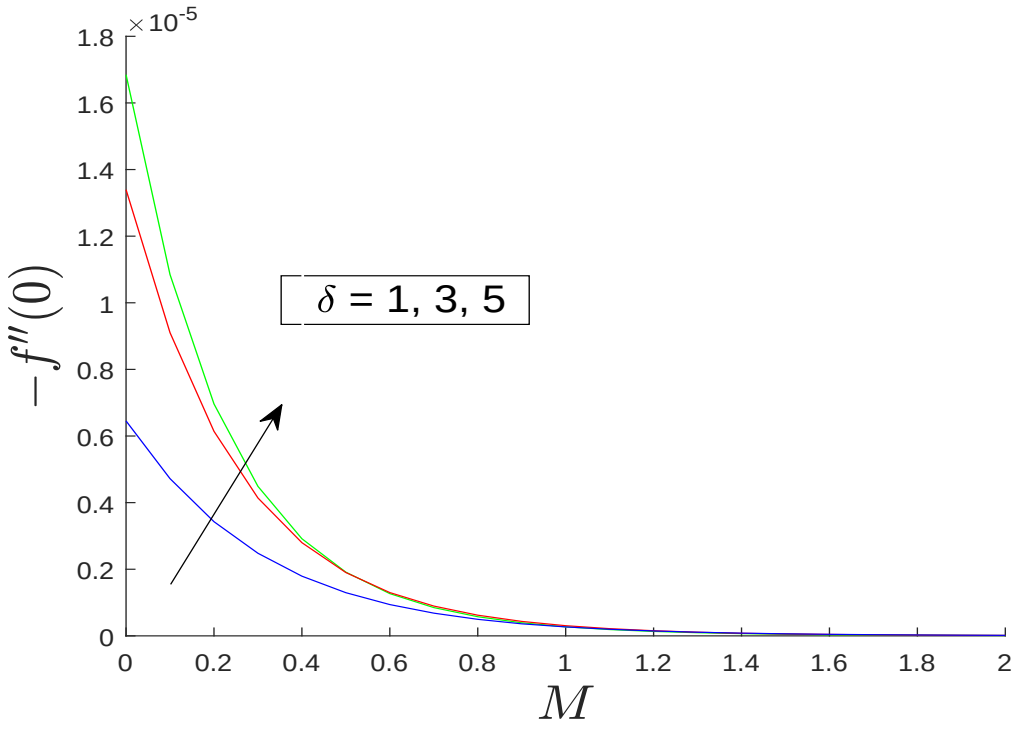

FIGURE 3.16: "Impact of δ on $-f''(0)$ when $Nb = Nt = 0.1$, $Pr = 2$, $A = 0.1$, $Bi = 10$, $\gamma = 10$"

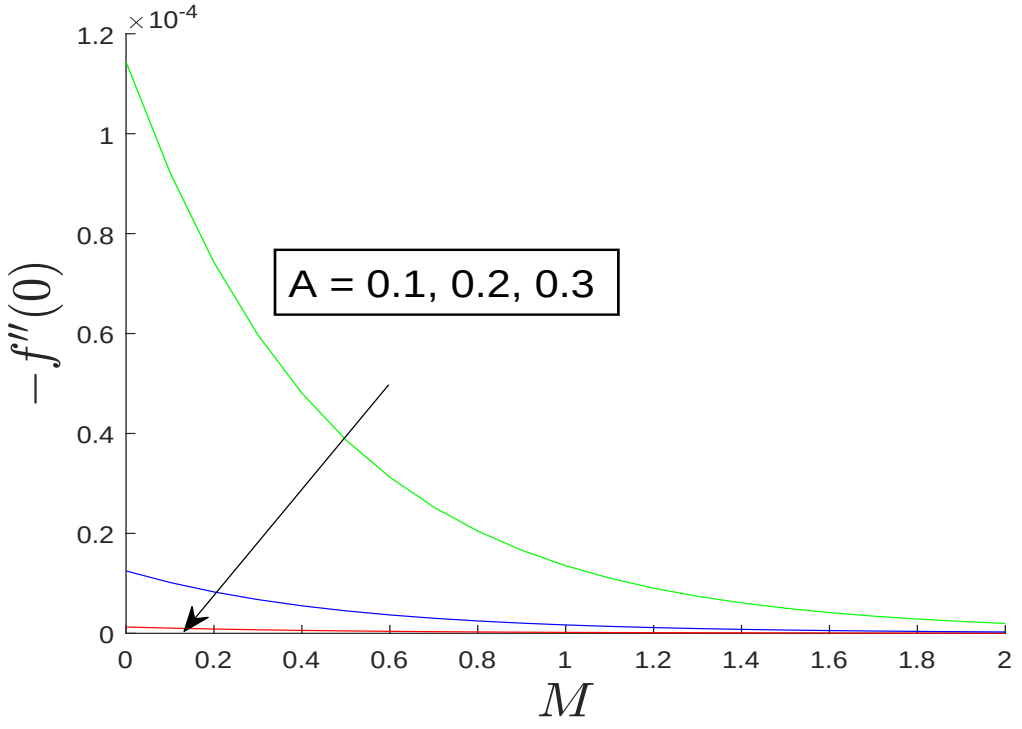

FIGURE 3.17: "Impact of A on $-f''(0)$ when $Nb = Nt = 0.1$, $Pr = 2$, $\delta = 1$, $Bi = 10$, $\gamma = 1$"

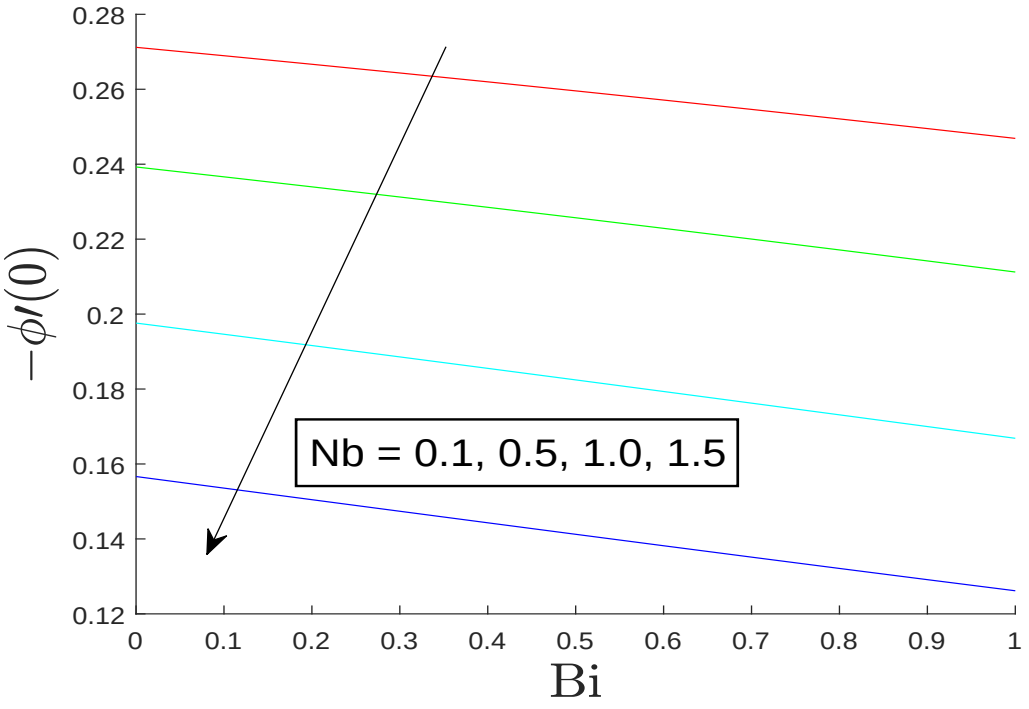

FIGURE 3.18: "Impact of Nb on $-\theta'(0)$ when $A = 0.4$, $Pr = M = 1$, $\delta = 0.2$, $\gamma = 0.1$"

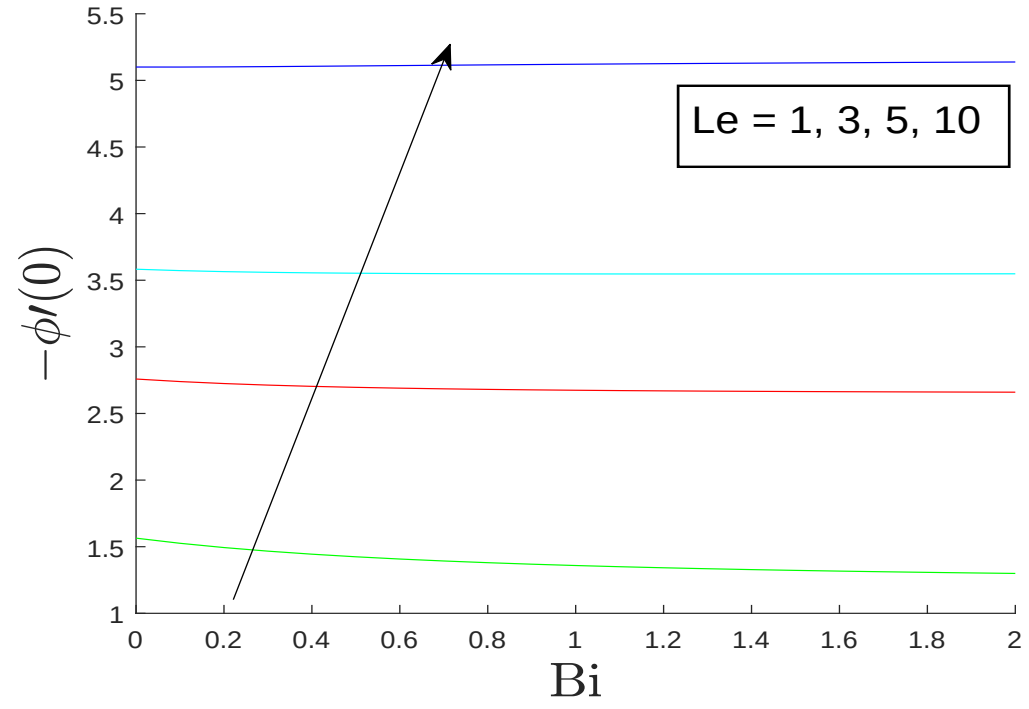

FIGURE 3.19: "Influence of Le on $-\phi'(0)$ when $Nb = Nt = 0.1$, $A = 0.4$, $Pr = 5$, $M = 1$, $\delta = 0.1$, $\gamma = 0.2$"

Chapter 4

Impact of Slip Wall on MHD Casson Nanofluid in the Presence of Viscous Dissipation and Thermal Radiation

4.1 Introduction

This chapter describes the flow of Casson nanofluid due to a linear stretch sheet along with the slip wall. Mechanism of heat and mass transport is also performed in the existence of Brownian motion and thermophoretic diffusion effect. Through an effective transformation, the PDEs are converted into dimensionless ODEs. To obtain the numerical solution for the considered model, shooting technique has been introduced. Numerical solutions are acquired for the velocity, temperature, and concentration profiles. The behavior of few pertinent emerging flow parameters are portrayed graphically. In addition, physical quantities are shown graphically. A detailed review work of Ibrahim and Makinde [25] has been presented in this chapter.

4.2 Mathematical Modeling

This chapter explains the 2-D stagnation point flow of MHD Casson nanofluid over an extending sheet under the impact of slip wall. An applied magnetic field of strength B_0 is applied perpendicular to the fluid motion. Additionally consider the impacts of Brownian motion and thermophoretic diffusion. Furthermore, the equations of energy and mass transport are also known to determine the profiles of temperature and concentration. The Cartesian coordinate system is regarded in such a way that x-axis is plated along the stretching plate and y- axis is normal. The stretching and slip velocities at the boundary are taken as $U_w(x) = ax$ and $U_{slip} = \left(\mu_B + \frac{P_y}{\sqrt{2\pi_c}}\right)\frac{\partial u}{\partial y}$ respectively, and C_w is the concentration at the wall, where $U_\infty = bx$, T_∞ and C_∞ represents the free stream velocity, temperature and concentration. Here T_w is the surface temperature. The graphical view of physical model is dispensed in Figure 4.1.

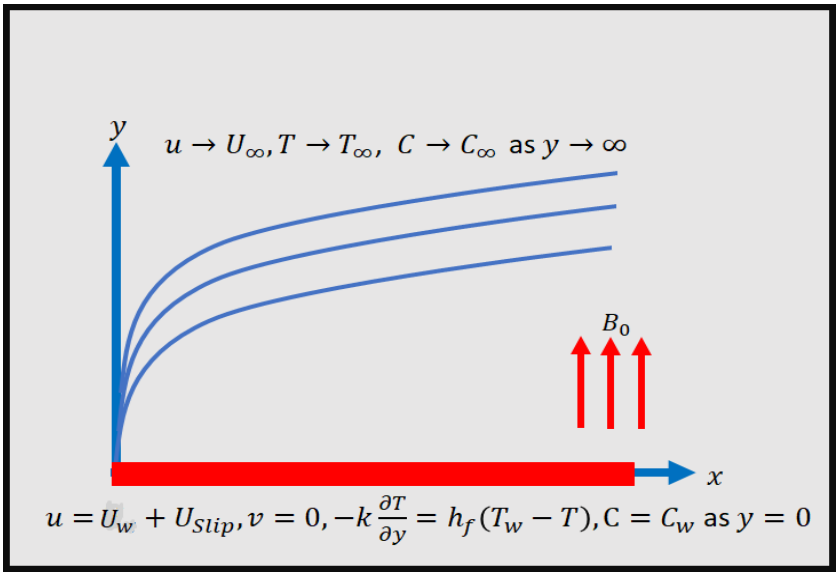

FIGURE 4.1: "Physical representation of the problem"

$$\frac{\partial u}{\partial x} + \frac{\partial v}{\partial y} = 0, \tag{4.1}$$

$$u\frac{\partial u}{\partial x} + v\frac{\partial u}{\partial y} = \nu\left(1 + \frac{1}{\gamma}\right)\frac{\partial^2 u}{\partial y^2} + U_\infty\frac{\partial U_\infty}{\partial x} + \frac{\sigma B_0^2}{\rho_f}(U_\infty - u), \tag{4.2}$$

$$u\frac{\partial T}{\partial x} + v\frac{\partial T}{\partial y} = \alpha\frac{\partial^2 T}{\partial y^2} + \Gamma\left[D_B\frac{\partial C\partial T}{\partial y\partial y} + \frac{D_T}{T_\infty}\left(\frac{\partial T}{\partial y}\right)^2\right] + \frac{\nu}{C_p}\left(1+\frac{1}{\gamma}\right)\left(\frac{\partial u}{\partial y}\right)^2 - \frac{1}{(\rho C)_f}\frac{\partial q_r}{\partial y}, \tag{4.3}$$

$$u\frac{\partial C}{\partial x} + v\frac{\partial C}{\partial y} = D_B\frac{\partial^2 C}{\partial y^2} + \frac{D_T\partial^2 T}{T_\infty\partial y^2} - K_0(C - C_\infty). \tag{4.4}$$

The related boundary conditions can be described as:

$$\left.\begin{aligned} &u = U_{w(x)} + U_{Slip} \rightarrow u = ax + \left(\mu_B + \frac{P_y}{\sqrt{2\pi_c}}\right)\frac{\partial u}{\partial y},\\ &v = 0, \quad -k\frac{\partial T}{\partial y} = h_f(T_f - T), \quad C = C_w \quad \text{at} \quad y = 0,\\ &u \rightarrow U_\infty = bx, \quad v = 0, \quad T \rightarrow T_\infty,\\ &C \rightarrow C_\infty \quad \text{as} \quad y \rightarrow \infty \end{aligned}\right\} \tag{4.5}$$

Here, u and v are components of velocity in the direction of x and y respectively, ρ_f is the fluid density, σ denotes the electrical conductivity, T represents the temperature, α is the thermal diffusivity, Γ represents the relation among heat capacity of the antiparticle and the liquid, C is the concentration parameter, μ_B represents the dynamic viscosity, P_y denotes the yield stress, π_c represents the critical value of product, k denotes the thermal conductivity, h_f denotes the coefficient of heat transfer and a and b are positive constant.

4.2.1 Similarity Transformation

This section introduced the similarity transformation.

$$\left.\begin{aligned} &\eta = y\sqrt{\frac{a}{\nu}}, \qquad \psi = \sqrt{a\nu}xf(\eta),\\ &\theta(\eta) = \frac{T - T_\infty}{T_w - T_\infty}, \quad \phi(\eta) = \frac{C - C_\infty}{C_w - C\infty}. \end{aligned}\right\} \tag{4.6}$$

The point by point procedure for the verification of the continuity Eqn. (4.1) has been examined in 3. For the conversion of (4.2)-(4.4) into the dimensionless form

has been depicted in the upcoming discussion.

As,

$$\theta(\eta) = \frac{T - T_\infty}{T_w - T_\infty},$$

$$T = T\infty + (T_w - T_\infty)\theta(\eta),$$

$$\frac{\partial T}{\partial x} = 0 + (T_w - T_\infty)\theta' \frac{\partial \eta}{\partial x}, \qquad \because \left(\frac{\partial \eta}{\partial x} = 0\right),$$

- $$\frac{\partial T}{\partial y} = 0 + (T_w - T_\infty)\theta' \frac{\partial \eta}{\partial y},$$

$$\frac{\partial \eta}{\partial y} = \sqrt{\frac{a}{\nu}}(T_w - T\infty)\theta',$$

- $$\frac{\partial^2 T}{\partial y^2} = \sqrt{\frac{a}{\nu}}(T_w - T\infty)\theta'' \frac{\partial \eta}{\partial y},$$

$$\frac{\partial^2 T}{\partial y^2} = \sqrt{\frac{a}{\nu}}(T_w - T\infty)\theta'' \sqrt{\frac{a}{\nu}}, \qquad \because \left(\frac{\partial \eta}{\partial y} = \sqrt{\frac{a}{\nu}}\right).$$

$$\frac{\partial^2 T}{\partial y^2} = \frac{a(T_w - T_\infty)}{\nu}\theta'', \tag{4.7}$$

Also,

$$\phi(\eta) = \frac{C - C_\infty}{C_w - C_\infty}, \tag{4.8}$$

- $C = C_\infty + (C_w - C_\infty)\phi(\eta),$

$$\frac{\partial C}{\partial x} = 0 + (C_w - C_\infty)\phi' \frac{\partial \eta}{\partial x},$$

$$\frac{\partial C}{\partial x} = 0, \qquad \because \left(\frac{\partial \eta}{\partial x} = 0\right)$$

- $$\frac{\partial C}{\partial y} = 0 + (C_w - C_\infty)\phi' \frac{\partial \eta}{\partial y},$$

$$= \sqrt{\frac{a}{\nu}}\,(C_w - C_\infty)\phi',$$

- $$\frac{\partial^2 C}{\partial y^2} = \sqrt{\frac{a}{\nu}}\,(C_w - C_\infty)\phi'' \frac{\partial \eta}{\partial y},$$

$$= \frac{a}{\nu}(C_w - C_\infty)\phi''. \tag{4.9}$$

Also

$$\bullet \quad \frac{\partial u}{\partial y} = \frac{\partial (axf')}{\partial y}, \\ = axf'' \cdot \frac{\partial \eta}{\partial y}, \\ = \frac{\partial a^3 x^2}{\nu} \cdot (f'')^2. \tag{4.10}$$

The expression qr is for radiative heat flux.

$$\bullet \quad q_r = -\frac{4\sigma^*}{3K_1}\frac{\partial T^4}{\partial y}. \tag{4.11}$$

Expanding T^4 to about T_∞,

$$T^4 = T_\infty^4 + 4T_\infty^3(T - T_\infty) + ...,$$

Ignoring the higher order terms

$$T^4 = 4T_\infty^3 T - 3T_\infty^4, \tag{4.12}$$

Using (4.12) in (4.11) we get,

$$= -\frac{4\sigma^*}{3K_1}\frac{\partial}{\partial y}(4T_\infty^3 T - 3T_\infty^4), \\ = -\frac{16\sigma^*}{3K_1}(T_\infty^3)\frac{\partial T}{\partial y}, \tag{4.13}$$

Using values of (4.11) and (4.13) in (4.3) we get

$$0 + (-\sqrt{a\nu}f)(\sqrt{\frac{a}{\nu}})(T_w - T_\infty)\theta' = \frac{\alpha\, a(T_w T_\infty)\theta''}{\nu} + \Gamma\frac{D_T}{T_\infty}\sqrt{\frac{a}{\nu}}\theta' \\ + \Gamma\, D_B\sqrt{\frac{a}{\nu}}(C_w - C_\infty)\phi' \cdot \sqrt{\frac{a}{\nu}}(T_w - T_\infty)\theta' \\ + \Gamma\frac{D_T}{T_\infty}\sqrt{\frac{a}{\nu}}(T_w - T_\infty)\theta'^2 + \frac{\nu}{C_p}(1 + \frac{1}{\gamma})\frac{a^3x^2}{\nu}(f'')^2 \\ - \frac{1}{(\rho C)_f}\frac{\partial}{\partial y}\left[(-\frac{16}{3k_1})\sigma^* T_\infty^3\frac{\partial T}{\partial y}\right],$$

$$
\begin{aligned}
-a(T_w - T_\infty) f\theta' =& \frac{\alpha\, a(T_w - T_\infty)\theta''}{\nu} + \frac{1}{(\rho C)_f}\frac{16}{3K_1}\Sigma^* T_\infty^3 \frac{\partial^2 T}{\partial y^2} \\
&+ \Gamma \frac{D_B}{\nu} a(C_w - C_\infty)(T_w - T_\infty)\phi'\theta' \\
&+ \Gamma \frac{a}{\nu}\frac{D_T}{T_\infty}(T_w - T_\infty)^2(\theta')^2 + \frac{\nu}{C_p}(1 + \frac{1}{\gamma})\frac{a^3x^2}{\nu}(f'')^2,
\end{aligned}
$$

$$
\begin{aligned}
-a(T_w - T_\infty) f\theta' =& \frac{\alpha\, a(T_w - T_\infty)\theta''}{\nu} + \frac{1}{(\rho C)_f}\frac{16}{3K_1}\Sigma^* T_\infty^3 \frac{a}{\nu}(T_w - T_\infty)\theta'' \\
&+ \Gamma \frac{D_B}{\nu} a(C_w - C_\infty)(T_w - T_\infty)\phi'\theta' \\
&+ \Gamma \frac{a}{\nu}\frac{D_T}{T_\infty}(T_w - T_\infty)^2(\theta')^2 + \frac{\nu}{C_p}(1 + \frac{1}{\gamma})\frac{a^3x^2}{\nu}(f'')^2, \qquad (4.14)
\end{aligned}
$$

Using $\Gamma = \frac{(\rho C)_p}{(\rho C)_f}$ in (4.14)

$$
\begin{aligned}
-a(T_w - T_\infty) f\theta' =& \frac{\alpha\, a(T_w - T_\infty)\theta''}{\nu} + \frac{(\rho C)_p}{(\rho C)_f}\frac{a}{\nu} D_B (C_w - C_\infty)(T_w - T_\infty)\phi'\theta' \\
&+ \frac{a}{\nu}\frac{D_T}{T_\infty}(T_w - T_\infty)^2(\theta')^2 + \frac{\nu}{C_p}(1 + \frac{1}{\gamma})\frac{a^3x^2}{\nu}(f'')^2 \\
&+ \frac{1}{(\rho C)_f}\frac{16}{3K_1}\Sigma^* T_\infty^3 \frac{a}{\nu}(T_w - T_\infty)\theta'', \qquad (4.15)
\end{aligned}
$$

Multiply each term of (4.15) by $\frac{\nu}{\alpha\, a(T_w - T_\infty)}$

$$
\begin{aligned}
-\frac{\nu}{\alpha} f\theta' =& \theta'' + \frac{(\rho C)_p}{(\rho C)_f\, \alpha} D_B (C_w - C_\infty)\phi'\theta' + \frac{(\rho C)_p}{(\rho C)_f\, \alpha}\frac{D_T}{T_\infty}(T_w - T_\infty)(\theta')^2 \\
&+ \frac{a^2x^2}{C_p(T_w - T_\infty)}\frac{\nu}{\alpha}(1 + \frac{1}{\gamma})(f'')^2 + \frac{1}{(\rho C)_f}\frac{16}{3K_1}\sigma^* T_\infty^3 \frac{1}{\alpha}\theta'',
\end{aligned}
$$

So

$$
\begin{aligned}
-P_r f\theta' =& \theta'' + \frac{(\rho C)_p}{\alpha(\rho C)_f} D_B (C_w - C_\infty)\phi'\theta' \\
&+ \frac{(\rho C)_p}{(\rho C)_f} D_T (T_w - T_\infty)(\theta')^2 \\
&+ \frac{a^2x^2}{C_p(T_w - T_\infty)} \cdot \frac{\nu}{\alpha}(1 + \frac{1}{\gamma})(f'')^2 \\
&+ \frac{1}{K}\frac{16}{3k_1}\sigma^* T_\infty^3 \theta'', \qquad (4.16)
\end{aligned}
$$

Multiplying and dividing of (4.16) by $\frac{\nu}{\nu}$

$$-P_r f\theta' = \theta'' + \frac{\nu}{\alpha}\frac{(\rho C)_p}{\nu(\rho C)_f}D_B(C_w - C_\infty)\phi'\theta' + \frac{\nu}{\alpha}\frac{(\rho C)_p}{(\rho C)_f}\frac{D_T}{T_\infty}(T_w - T_\infty)(\theta')^2 + \frac{a^2x^2}{C_p(T_w - T_\infty)}\cdot\frac{\nu}{\alpha}(1+\frac{1}{\gamma})(f'')^2 + \frac{16}{3Kk_1}\sigma^* T_\infty^3\theta''. \tag{4.17}$$

As,

$$N_b = \frac{(\rho C)_p D_B(C_w - C_\infty)}{(\rho C)_f \nu}, \quad N_t = \frac{(\rho C)_p D_T(T_w - T_\infty)}{(\rho C)_f \nu T_\infty} \tag{4.18}$$

And

$$\frac{4}{3}\frac{4}{kk_1}\Sigma^* T_\infty^3\theta'',$$

$$\begin{aligned} R &= \frac{kk_1}{4\sigma^* T_\infty^3}, \\ \frac{1}{R} &= \frac{4\Sigma^* T_\infty^3}{kk_1}, \\ \frac{1}{R} &= \frac{4}{3R}\theta''. \end{aligned} \tag{4.19}$$

As,

$$E_c = \frac{U_w^2}{C_p(T_w - T_\infty)}, \tag{4.20}$$

Using values of (4.18), (4.19) and (4.20) in (4.17) then (4.17) becomes,

$$\begin{aligned} -P_r f\theta' &= \theta'' + N_b P_r \phi'\theta' + N_t P_r(\theta')^2 + E_c P_r(1+\frac{1}{\gamma})(f'')^2 + \frac{4}{3R}\theta'', \\ \theta'' + P_r f\theta' + N_b P_r\phi'\theta' + N_t P_r(\theta')^2 + E_c P_r(1+\frac{1}{\gamma})(f'')^2 + \frac{4}{3R}\theta'' &= 0, \\ (1+\frac{4}{3R})\theta'' + P_r f\theta' + P_r N_b\phi'\theta' + N_t P_r(\theta')^2 + E_c P_r(1+\frac{1}{\gamma})(f'')^2. \end{aligned} \tag{4.21}$$

Using all converted expressions in (4.4)

$$0 + (-\sqrt{a\nu}f)\cdot\sqrt{\frac{a}{\nu}}f(C_w - C_\infty)\phi' = D_B\frac{a}{\nu}(C_w - C_\infty)\phi'' + \frac{D_T}{T_\infty}\frac{a}{\nu}(T_w - T_\infty)\theta'' - k_0[(C_w - C_\infty)\phi + C_\infty - C_\infty],$$

$$-\sqrt{a\nu\frac{a}{\nu}}(C_w - C_\infty)f\phi' = \frac{D_B}{\nu}a(C_w - C_\infty)\phi'' + \frac{D_T}{T_\infty}\frac{a}{\nu}(T_w - T_\infty)\theta'' - k_0[(C_w - C_\infty)\phi],$$

$$-a(C_w - C_\infty)f\phi' = \frac{D_B}{\nu}a(C_w - C_\infty)\phi'' + \frac{D_T}{T_\infty}\frac{a}{\nu}(T_w - T_\infty)\theta'' - k_0[(C_w - C_\infty)\phi]. \tag{4.22}$$

Multiplying each term of (4.22) by $\frac{\nu}{a\,D_B(C_w - C_\infty)}$

$$-\frac{\nu}{D_B}f\phi' = \phi'' + \frac{D_T}{D_B T_\infty}\frac{(T_w - T_\infty)}{(C_w - C_\infty)}\theta'' - \frac{\nu(C_w - C_\infty)}{aD_B(C_w - C_\infty)}\phi\, k_0, \tag{4.23}$$

As,

$$\begin{aligned} L_e P_r &= \frac{\alpha}{D_B}\cdot\frac{\nu}{\alpha}, \\ L_e P_r &= \frac{\nu}{D_B}, \end{aligned} \tag{4.24}$$

And

$$\begin{aligned} \frac{N_t}{N_b} &= \frac{(\rho C)_p D_T(T_w - T_\infty)}{(\rho C)_f \nu T_\infty} \div \frac{(\rho C)_p D_B(C_w - C_\infty)}{(\rho C)_f \nu}, \\ &= \frac{(\rho C)_p D_T(T_w - T_\infty)}{(\rho C)_f \nu T_\infty} \times \frac{(\rho C)_f \nu}{(\rho C)_p D_B(C_w - C_\infty)}, \\ &= \frac{D_T(T_w - T_\infty)}{D_B T_\infty(C_w - C_\infty)}, \end{aligned} \tag{4.25}$$

Using (4.24) and (4.25) in (4.23) we get

$$\begin{aligned} -\frac{\nu}{D_B}f\phi' &= \phi'' + \frac{D_T(T_w - T_\infty)}{D_B T_\infty(C_w - C_\infty)}\theta'' - \frac{\nu}{aD_B}\phi k_0, \\ -L_e P_r f\phi' &= \phi'' + \frac{N_t}{N_b}\theta'' - L_e\frac{1}{a}\phi k_0 && \because \left(L_e = \frac{\nu}{D_B}\right) \\ \phi'' + L_e P_r f\phi' &+ \frac{N_t}{N_b}\theta'' - L_e\frac{k_0}{a}\phi = 0 && \because \left(k = \frac{k_0}{a}\right). \end{aligned}$$

The detailed procedure for the conversion of equations (4.3)-(4.4) and boundary conditions into the dimensionless form is similar to that discussed in (3). Finally,

the ODEs describing the proposed ow problem can be re-collected in the following system.

$$(1+\frac{4}{3R})\theta^{''}+P_r f\theta^{'}+P_r N_b\phi^{'}\theta^{'}+N_t P_r(\theta^{'})^2+E_c P_r(1+\frac{1}{\gamma})(f^{''})^2 \tag{4.26}$$

$$\phi^{''}+L_e P_r f\phi^{'}+\frac{N_t}{N_b}\theta^{''}-L_e\frac{k_0}{a}\phi=0. \tag{4.27}$$

The transform boundary conditions are stated below:

$$\left.\begin{aligned} &f(0)=0,\\ &f^{'}(0)=1+\delta\left(1+\frac{1}{\gamma}\right)f^{''}(0),\\ &\theta^{'}(0)=-B_i[1-\theta(0)], \qquad \phi(0)=1, \quad \text{at} \quad \eta=0,\\ &f^{'}(\infty)\to A, \qquad \theta(\infty)\to 0, \qquad \phi(\infty)\to 0, \quad as \quad \eta\to\infty. \end{aligned}\right\} \tag{4.28}$$

The description of different parameters used in the above equations shall be as follows:

$$\left.\begin{aligned} A&=\frac{b}{a},\\ Pr&=\frac{\nu}{\alpha},\\ M&=\frac{\sigma B_0^2}{\rho_f a},\\ \delta&=\mu_\beta\sqrt{\frac{a}{\nu}},\\ Le&=\frac{\alpha}{D_B},\\ Bi&=\frac{h_f}{k}\sqrt{\frac{\nu}{a}},\\ Nb&=\frac{(\rho C)_p}{(\rho C)_f\nu}D_B(C_w-C_\infty),\\ Nt&=\frac{(\rho C)_p}{(\rho C)_f\nu}D_T(T_w-T_\infty). \end{aligned}\right\} \tag{4.29}$$

The skin friction coefficient, is given as follows:

$$C_f=\frac{\tau_w}{\rho u_w^2}, \tag{4.30}$$

where

$$\begin{aligned}\tau_w &= \left(\mu_B + \frac{P_y}{\sqrt{2\pi_c}}\right)\left(\frac{\partial u}{\partial y}\right),\\ &= \mu\left(1 + \frac{P_y}{\mu\sqrt{2\pi_c}}\right)\left(\frac{\partial u}{\partial y}\right),\\ &= \tau\mu_B\left(1 + \frac{1}{\gamma}\right)\frac{\partial u}{\partial y}, \qquad (4.31)\end{aligned}$$

$$u_w(x) = ax, \qquad (4.32)$$

$$\begin{aligned}\frac{\partial u}{\partial y} &= axf''\sqrt{\frac{a}{\nu}},\\ &= a\sqrt{\frac{a}{\nu}}xf'', \qquad (4.33)\end{aligned}$$

Using Eqn. (4.33) in (4.31) and (4.31) in (4.30) , we get

$$C_f = \frac{\mu_B\left(1 + \frac{1}{\gamma}\right)a\sqrt{\frac{a}{\nu}}xf''}{\rho a^2x^2},$$

$$\begin{aligned}&= \frac{\frac{\nu}{\sqrt{\nu}}\left(1 + \frac{1}{\gamma}\right)a\sqrt{a}xf''}{a^2x^2},\\ &= \frac{\frac{\nu}{\sqrt{\nu}}\left(1 + \frac{1}{\gamma}\right)a\sqrt{a}xf''}{ax},\\ &= \frac{\sqrt{\nu}}{\sqrt{a}x}\left(1 + \frac{1}{\gamma}\right)f'', \qquad (4.34)\\ C_f\frac{\sqrt{a}}{\sqrt{\nu}}\sqrt{x}\sqrt{x} &= \left(1 + \frac{1}{\gamma}\right)f'',\\ C_f\frac{\sqrt{ax}}{\sqrt{\nu}}\sqrt{x} &= \left(1 + \frac{1}{\gamma}\right)f'',\\ C_f\frac{\sqrt{u_w}\sqrt{x}}{\sqrt{\nu}} &= \left(1 + \frac{1}{\gamma}\right)f''. \qquad (4.35)\end{aligned}$$

As

$$Re_x = \frac{U_w.x}{\nu}, \qquad (4.36)$$

so

$$\begin{aligned} Re_x^{\frac{1}{2}} &= \frac{U_w^{\frac{1}{2}}.x^{\frac{1}{2}}}{\nu^{\frac{1}{2}}} \\ &= \frac{\sqrt{u_w}\sqrt{x}}{\sqrt{\nu}} \\ C_f Re_x^{\frac{1}{2}} &= \left(1+\frac{1}{\gamma}\right) f''. \end{aligned} \tag{4.37}$$

The local Nusselt number is specified as:

$$Nu_x = \frac{xq_w}{k(T_w - T_\infty)},$$

where

$$q_w = -k\left(\frac{\partial T}{\partial y}\right)_{y=0},$$

and

$$\frac{\partial T}{\partial y} = \sqrt{\frac{a}{\nu}}\left(T_w - T_\infty\right)\theta'(0) \tag{4.38}$$

Using Eqn. (4.38) in (4.38) and (4.38) in (4.38)

$$\begin{aligned} Nu_x &= -x\sqrt{\frac{a}{\nu}} \quad \theta'(0) \\ \Rightarrow \; Nu_x &= -\frac{\sqrt{x}\sqrt{x}\sqrt{a}}{\theta}{}'\sqrt{\nu} \\ \Rightarrow \; Nu_x &= -\frac{\sqrt{x}\sqrt{ax}}{\theta}{}'\sqrt{\nu} \\ \Rightarrow \; Nu_x &= -\sqrt{Rex} \quad \theta'(0). \end{aligned} \tag{4.39}$$

The local Sherwood number is specified as:

$$Shx = \frac{xhm}{D_B}(C_w - C_\infty), \tag{4.40}$$

$$hm = -D_B\left(\frac{\partial \phi}{\partial y}\right), \tag{4.41}$$

$$\begin{aligned} \frac{\partial \phi}{\partial y} &= (C_w - C_\infty)\phi'.\frac{\partial \eta}{\partial y} + 0, \\ &= \sqrt{\frac{a}{\nu}}(C_w - C_\infty)\phi', \end{aligned} \tag{4.42}$$

Using Eqn. (4.42) in Eqn. (4.38)

$$hm = -D_B\sqrt{\frac{a}{\nu}}(C_w - C_\infty)\phi^{'}(0), \tag{4.43}$$

Using Eqn. (4.43) in (4.41)

$$\begin{aligned} Shx &= -\frac{xDB\sqrt{\frac{a}{\nu}}(C_w - C_\infty)\phi^{'}(0)}{DB(C_w - C_\infty)}, \\ &= -x\sqrt{\frac{a}{\nu}} \qquad \phi^{'}(0), \\ &= \frac{-\sqrt{x}\sqrt{ax}\phi^{(0)}}{\sqrt{\nu}}, \\ &= -\sqrt{Rx} \quad \phi^{'}(0), \\ \Rightarrow \quad \frac{Shx}{\sqrt{Rx}} &= -\phi^{'}(0). \end{aligned} \tag{4.44}$$

4.3 Solution Technique

In order to solve the arrangement of ODEs (4.46)- (4.50) subject to the boundary conditions (4.51), the shooting technique has been used. Basically equation (4.46) is solved numerically and afterward the computed results of f, $f^{'}$ and $f^{''}$ are used in equations (4.47)-(4.50). For the numerical treatment of equation (4.46), the missing initial condition $f^{''}(0)$ has been denoted as p and the following notations

have been considered.

$$\begin{aligned} f &= g_1, \\ f' &= g_1' = g_2, \\ f'' &= g_1'' = g_2' = g_3, \\ \frac{\partial f}{\partial p} &= g_4, \\ \frac{\partial f'}{\partial p} &= g_5, \\ \frac{\partial f''}{\partial p} &= g_6, \end{aligned} \tag{4.45}$$

Using the above notes, equation (4.46) can be translated into a scheme of three first order ODEs. The reduced form of (4.46) is the first three of the ODEs, and the remaining three are obtained by differentiating the first three w.r.t p.

$$\begin{aligned} &g_1^{'} = g_2; && g_1(0) = 0 \\ &g_2^{'} = g_3; && g_2(0) = 1 + \delta\left(1 + \frac{1}{\gamma}\right)g \\ &g_3^{'} = \frac{\gamma}{\gamma+1}\left[-g_1 g_3 + g_2^2 - A^2 - M(A - g_2)\right]; && g_3(0) = p \\ &g_4^{'} = g_5; && g_4(0) = 0 \\ &g_5^{'} = g_6; && g_5(0) = \delta\left(1 + \frac{1}{\gamma}\right) \\ &g_6^{'} = \frac{\gamma}{\gamma+1}\left[-g_4 g_3 - g_1 g_6 + 2g_2 g_5 + M g_5\right]; && g_6(0) = 1 \end{aligned}$$

The RK-4 technique has been used to tackle the above initial value problem. In order to get the approximate numerical results , the problem's domain is considered to be bounded i.e $[0, \eta_\infty]$, where η_∞ is chosen to be an appropriate finite positive real number so that the variation in the result for $\eta \gg \eta_\infty$ is ignorable. The missing condition for the above system of equations is to be picked to such an extent that $(g_2(\infty))_p = A$. This mathematical equation was solved by using the technique of

the Newton as illustrated by the following iterative scheme.

$$p^{(n+1)} = p^{(n)} - \frac{(g_2(\eta_\infty))_{g=g^{(n)}} - A}{\left(\frac{\partial g_2(\eta_\infty)}{\partial g}\right)_{p=p^{(n)}}}, \tag{4.46}$$

$$p^{(n)} - \frac{(g_2(\eta_\infty))_{p=p^{(n)}} - A}{(g_2(\eta_\infty))_{p=p^{(n)}}}, \tag{4.47}$$

The stopping criteria for the shooting strategy is set as:

$$|(g_2(\eta_\infty)) - A| \lessdot \epsilon, \tag{4.48}$$

for some sufficiently small positive number ϵ.

4.4 Results and Discussion

Within this section, the numerical solutions are discussed in detail using graphs and tables. We will primarily address the profile of velocity, temperature , and concentration. The present results will be compared with those of [25] for verification of the code. The numerical calculations are executed for the observation of the impact of relevant physical parameters like, Casson fluid parameter γ, slip parameter δ, velocity correlation parameter A, Biot number Bi, Brownian motion parameter Nb, thermophoresis parameter $N(t)$, Lewis number Le on the skin friction coefficient, Nusselt number, and Sherwood number. Such related physical parameters have an immediate effect on distributions of velocity, temperature , and concentration.

Table 4.1 shows the numerical results of the skin-friction coefficient along with Nusselt and sherwood numbers for the current model in respect of a shift in the values of various parameters such as A, δ, γ, Nb, Nt, Pr, Le, Bi, M, Ec, R and K. From the results it was noted that the skin-friction coefficient decreases for the larger values of A and δ, while heat and mass transfer rates increase significantly.

Table 4.2 portray the intervals I_f, I_θ and I_ϕ where from the missing initial conditions $f''(0)$, $\theta'(0)$ and $\phi'(0)$ respectively can be chosen. It is noteworthy that the intervals mentioned offer a considerable flexibility for the choice of initial guesses.

4.4.1 Influence of Casson Parameter on Skin Friction

Figure 4.2 is the graphical representation which depicts the γ on the velocity filed. The fluid velocity rises with escalating the values of γ. Physically the viscosity of the fluid increases due to enhancing the values of γ which in turn declines the velocity profile of the fluid, also for enlarging values of γ, the velocity boundary layer thickness diminishes. Furthermore, the present phenomenon change to Newtonian fluid when γ tends to infinity.

4.4.2 Impact of Slip Parameter on Skin Friction

Figure 4.3 exhibits the influence of δ on the dimensionless velocity distribution. It is clearly manifest the velocity profile escalates by mounting values of δ. Generally, the growing values of δ create a frictional resistance between the surface of the sheet and fluid particles enhance, which causes a decrement of the fluid velocity.

4.4.3 Impact of Velocity Ratio on Skin Friction Parameter

Figure 4.4 analyzes the effect of A on the distribution of dimensionless velocity. From the figure it is apparent that when the free stream velocity is greater than the surface velocity, while the fluid particle velocity accelerates at $A > 1$. In addition the thickness of the boundary layer decelerates by increasing the A values. In fact, if the stretching velocity is less than the free-stream velocity the velocity graph tends to be A. Often, when the stretching sheet velocity is greater than the free-stream velocity, which creates a fluid velocity declaration.

4.4.4 Biot Number Impact on Temperature Profile

Figure4.5 demonstrates the effect of Bi on the dimensionless temperature distribution. The graph of the velocity profile demonstrate that an enlargement in Bi causes an enhancement in the temperature profile. Generally, Biot number can be expressed as the ratio of convection at the surface to conduction within the surface of the body. As expected, the boosting values of Bi enhanced the thermal boundary layer of the fluid.

4.4.5 Temperature Profile Under The Effect of Brownian Motion

Figure 4.6 depicts the impact of Nb on the temperature profile. The temperature distribution enhances with the uprising values of Nb. It is observed that a inflated Nb strengthens the fluid temperature owing to more collisions between the fluid particles.

4.4.6 Thermophoresis Parameter Effects on Temperature Profile

Figure 4.7 portrays the effect of Nt on temperature distribution, the temperature field is obviously improved from the calculation for step by step extending values of Nt. In addition, the particles Nt apply a force on the other particles because of which these particles shift from hotter to less region. Therefore, there is an enhancement in the fluid's temperature profile.

4.4.7 Impact of Temperature Profile on Slip Parameter

Figure 4.8 delineates the impact of δ on temperature distribution, from the figure clearly for step by step growing values of δ the temperature field is decline.

Furthermore, the thermal boundary layer thickness is reduced. Moreover the temperature boundary layer thickness also shows a declining behavior.

4.4.8 Effect of Parameter Velocity Ratio on Temperature Profile

Figure 4.9 illustrates the impact of A on dimensionless temperature profile. We see that for boosting values of A the temperature distribution declines. Moreover, increasing the values of A by which the thermal boundary layer thickness diminishes.

4.4.9 Casson Parameter Effect on Temperature Profile

Figure 4.10 displays the impact of γ on temperature distribution. The boosting values of γ escalating temperature profile. Generally the thermal boundary layer thickness build up by increasing values of γ due to which the surface temperature enlarge with γ.

4.4.10 Impact of Lewis Number on Profile of Concentration

Figure 4.11 shows the relationship between Lewis numbers and the dimensional concentration distribution. Concentration profile decelerate for the boosting values of Le and thus we have get a small molecular diffusivity and thermal boundary layer. Physically, concentration distribution is a reducing function of Lewis number.

4.4.11 Effect of Biot Number on Profile of Concentration

Figure 4.12 shows the relationship between Bi and the concentration profile. For boosting values of Bi the graph of dimensionless concentration profile is increased. Increasing Bi means a reduction in the conductivity of the fluid due to which the concentration boundary layer is enhanced.

4.4.12 Thermophoresis Effect Parameter on Concentration Profile

Figure 4.13 shows the effect of Nt on both temperature and concentration distribution, from the figure it is pellucid that both the θ temperature and the ϕ concentration area are enhanced for cautiously enlarging values of Nt. In Nt the particles actually apply a force on the other particles because of which these particles move from the hotter to less zone. Hence an boost in the fluid's θ and ϕ profile.

4.4.13 Impact of Casson Parameter on Profile of Concentration

Figure 4.14 exhibits the relationship between γ and concentration profile. Actually concentration of fluid and its associative boundary thickness are increases by mounting values of γ. Figures [4.15]-[4.17] are sketched to demonstrate the effect of skin friction coefficient against magnetic parameter to increase values of Casson parameter, slip parameter and velocity ratio parameter.

4.4.14 Impact of Casson Parameter on Skin Friction

It is noted in Figure 4.15 that with an increase in the Casson fluid parameter the skin friction coefficient decreases significantly, which implies that the drag forces on the surface reduces effectively.

4.4.15 Effect on Skin Friction by Slip Parameter

Figure 4.16 reflect that with an increase in the slip parameter the skin friction coefficient increases effectively.

4.4.16 Effect of Parameter Velocity Ratio on The Skin Friction

Figure 4.17 displays that that with an enhancement in velocity ratio parameter the skin friction coefficient reduces effectively.

4.4.17 Impact on Nusselt Number of The Brownian Motion Parameter

Figure 4.18 shows the impact of Nb on Nu_x plotted against Nt. As the estimations of the two parameters Nt and Nb increases, the nearby Nu_x decreases.

4.4.18 Lewis Number Effect on Sherwood Number

Figure 4.19 displays the impact of Le on Sh_x as for Biot number. It is seen that local sherwood number rises with an increment in the Lewis number. It can be noted that, the field Nu_x is also increased by enhancing the values of Le whenever the N_ux extends; as the values of Bi as well increases the nearby Sh_x decreases.

TABLE 4.1: The computed results of skin friction coefficient, Nusselt and Sherwood numbers for various estimations of δ and γ and A and E_c and R and K. When "$N_b = N_t = 0.1, Pr = Le = 10, Bi = 0.1$, and $M = 1$".

A	δ	γ	E_c	R	k	$-f''(0)$	$-\theta'(0)$	$-\phi'(0)$
0.0	0.1	10	0.1	0.1	0.5	1.1415	0.0731	7.5077
0.1	—	—	—	—	—	1.0653	0.0745	7.5646
0.2	—	—	—	—	—	0.9792	0.0748	7.6278
0.3	—	—	0.5	0.7	1.5	0.8838	0.0237	7.6278
0.9	—	—	—	—	—	0.1467	-0.0615	8.4417
1.5	—	—	1.0	1.0	—	-0.8188	-0.4864	8.9666
2.0	—	—	—	—	—	-1.7623	-0.0724	10.8472
2.4	—	—	—	—	—	-2.5944	-0.9483	11.4924
0.4	0.2	—	—	—	—	0.6758	-0.0775	8.5189
—	0.4	—	—	—	—	0.5357	-0.0669	8.1344
—	0.6	—	—	—	—	0.4449	-0.0602	7.8735
—	0.8	—	—	—	—	0.3810	-0.0556	7.6835
—	0.4	0.1	—	0.1	—	0.0908	-0.8725	7.7625
—	—	0.5	—	1.0	—	0.2563	-0.4145	8.4529
—	—	1	—	—	—	0.3477	-0.2163	8.2658
—	—	10	—	—	—	0.5357	-0.0669	8.1344
—	—	10	—	—	—	0.5688	-0.0531	8.1244

TABLE 4.2: The intervals for the initial guesses for the missing initial conditions when "$N_b = N_t = 0.1$, $Pr = Le = 10$, $Bi = 0.1$, and $M = 1$".

A	δ	γ	E_c	R	k	I_f	I_θ	I_ϕ
0.0	0.1	10	0.1	0.1	0.5	[-0.5,0.5]	[-4.5,4.5	[-4.5,9.2]
0.1	—	—	—	—	—	[-0.9,0.5]	[-5.5,1.9]	[-6.5,7.5]
0.2	—	—	—	—	—	[-0.5,0.7]	[-9.5,8.5]	[-9.5,7.5]
0.3	—	—	0.5	0.7	1.5	[-0.7,0.7]	[-9.2,7.5]	[-9.2,8.5]
0.9	—	—	—	—	—	[-0.1,1.3]	[-3.9,4.5]	[-9.9,5.8]
1.5	—	—	1.0	1.0	1.5	[1.0,1.3]	[-4.9,3.9]	[-4.9,4.9]
2.0	—	—	—	—	—	[1.8,2.2]	[-3.9,2.9]	[-3.9,2.9]
2.4	—	—	—	—	—	[2.5,3.1]	[-4.5,4.5]	[-4.5,3.5]
0.4	0.2	—	—	—	—	[-0.5,0.5]	[-9.5,7.5]	[-9.5,8.5]
—	0.4	—	—	0.1	—	[-0.3,0.4]	[-9.8,9.9]	[-9.8,9.9]
—	0.6	—	—	1.0	—	[-0.3,0.2]	[-5.9,8.9]	[-5.9,9.7]
—	0.8	—	—	—	—	[-0.4,0.1]	[-6.6,7.6]	[-6.5,5.5]
—	0.4	0.1	—	—	—	[-0.3,0.3]	[-5.5,7.9]	[-5.5,9.9]
—	—	0.5	—	—	—	[-0.3,2]	[-9.9,8.6]	[-9.8,9.8
—	—	1	—	—	—	[-0.4,1.4]	[-8.5,7.5]	[-8.5,6.5]
—	—	10	—	—	—	[-0.5,1.5]	[-3.9,1.9]	[-3.9,2.9]
—	—	10	—	—	—	[-0.5,1.6]	[-4.9,1.8]	[-4.9,3.9]

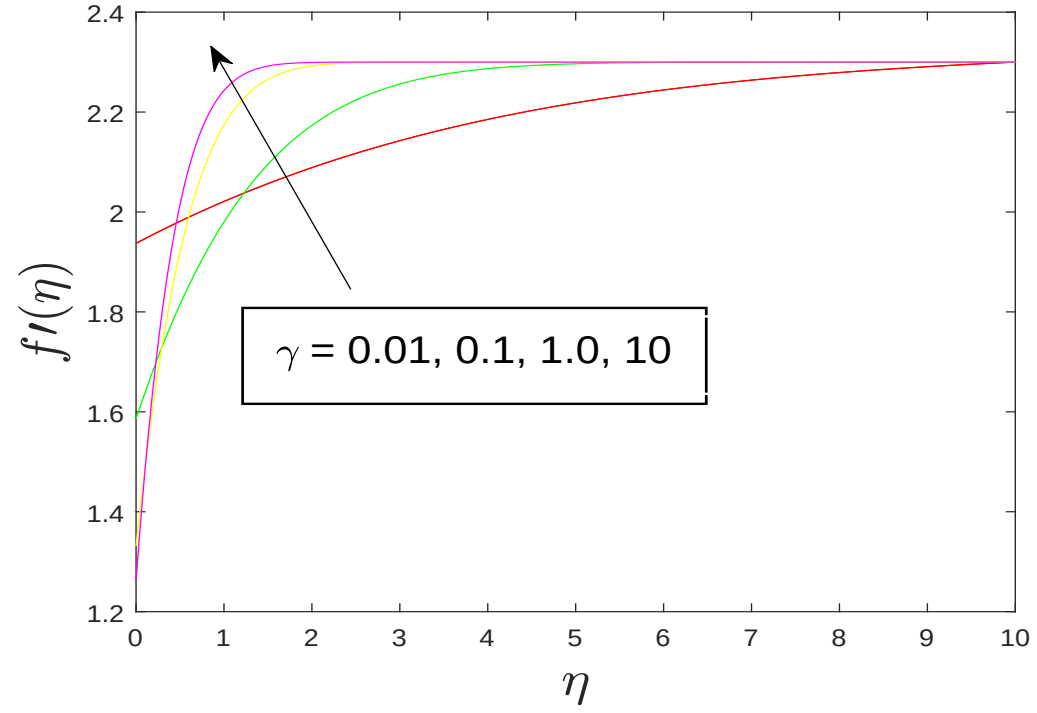

FIGURE 4.2: "Effect of γ on $f'(\eta)$ when $\delta = 0.1$, $A = 2.3$, $Pr = M = 1$, $Nb = Nt = 0.5$, $Le = 2$, $Bi = 0.5$, $R = 0.5$, $K = 0.5$, $Ec = 0.1$"

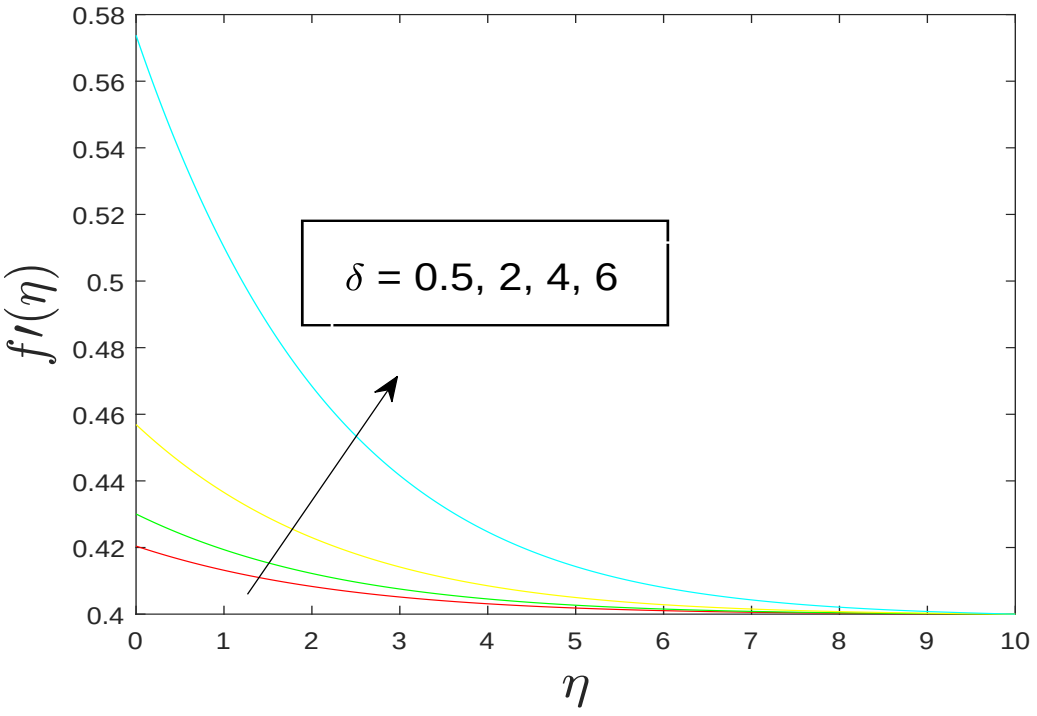

FIGURE 4.3: "Effect of δ on $f'(\eta)$ when $\gamma = 0.1$, $A = 0.4$, $Pr = M = 1$, $Nb = Nt = 0.5$, $Le = 2$, $Bi = 0.5$, $R = 0.5$, $K = 0.5$, $Ec = 0.1$"

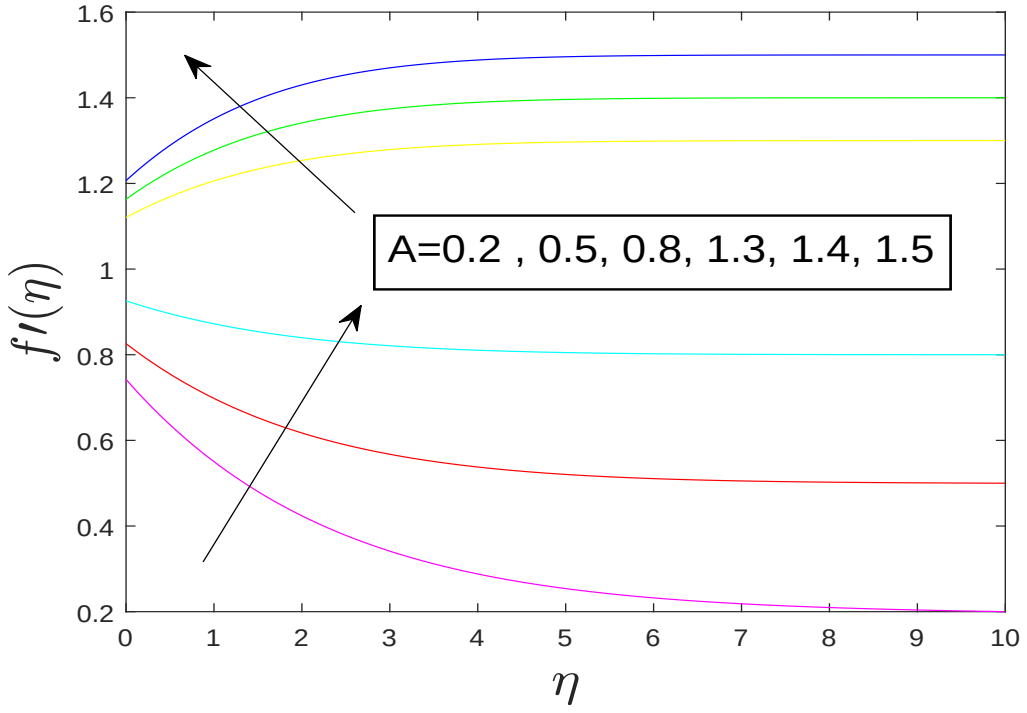

FIGURE 4.4: "Effect of A on $f'(\eta)$ when $\gamma = 0.1$, $\delta = 0.1$, $Pr = M = 1$, $Nb = Nt = 0.5$, $Le = 2$, $Bi = 0.5$, $R = 0.5$, $K = 0.5$, $Ec = 0.1$"

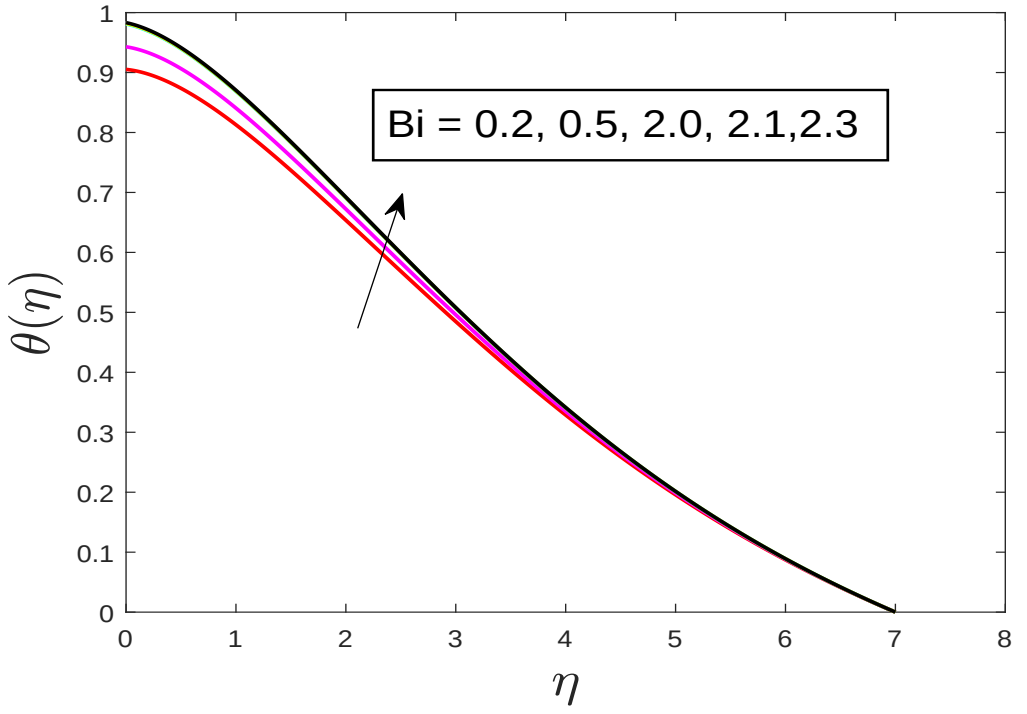

FIGURE 4.5: "Impact of Bi on $\theta(\eta)$ when $Nb = Nt = 0.5$,$Le = 2$, $\gamma = 0.1$, $\delta = 0.2$, $Pr = M = 1$, $A = 0.4$, $R = 0.5$, $K = 0.5$, $Ec = 0.1$"

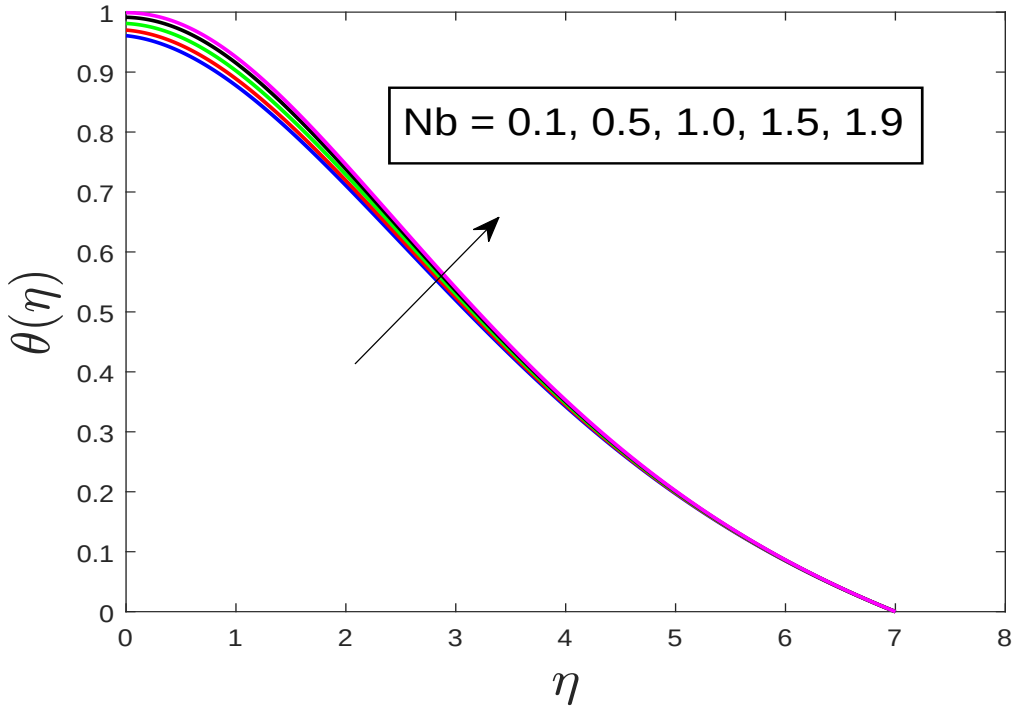

FIGURE 4.6: "Impact of Nb on $\theta(\eta)$ when $Nt = 0.5$, $Le = 2$, $\gamma = 0.1$, $\delta = 0.2$, $Pr = M = 1$, $A = 0.4$, $R = 0.5$, $K = 0.5$, $Ec = 0.1$"

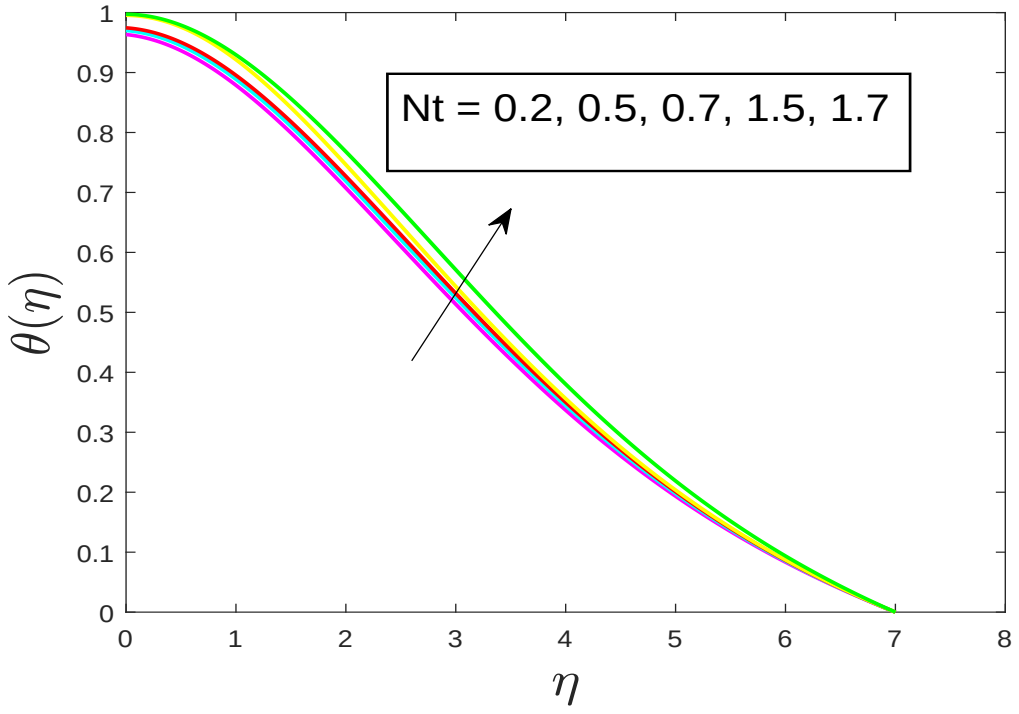

FIGURE 4.7: "Effect of Nt on $\theta(\eta)$ when $Nb = 0.5$, $Le = 2$, $\gamma = 0.1$, $Bi = 0.5$, $\delta = 0.2$, $Pr = M = 1$, $A = 0.4$, $R = 0.5$, $K = 0.5$, $Ec = 0.1$"

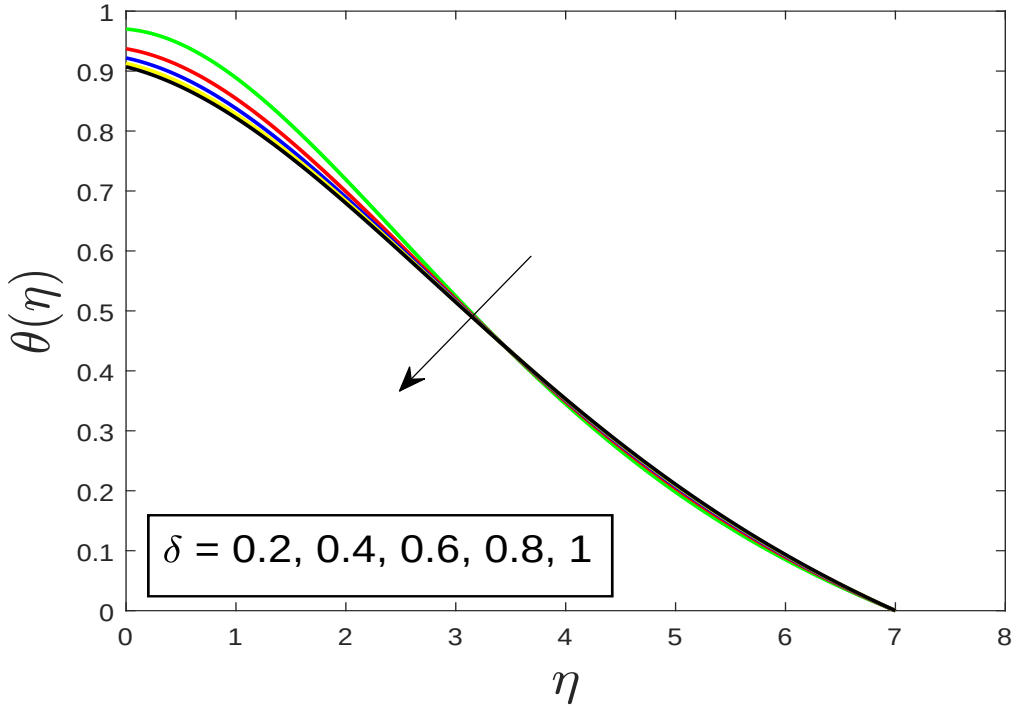

FIGURE 4.8: "Impact of δ on $\theta(\eta)$ when $Nb = Nt = 0.5$, $Le = 2$, $\gamma = 0.1$, $Bi = 0.5$, $Pr = M = 1$, $A = 0.4$, $R = 0.5$, $K = 0.5$, $Ec = 0.1$"

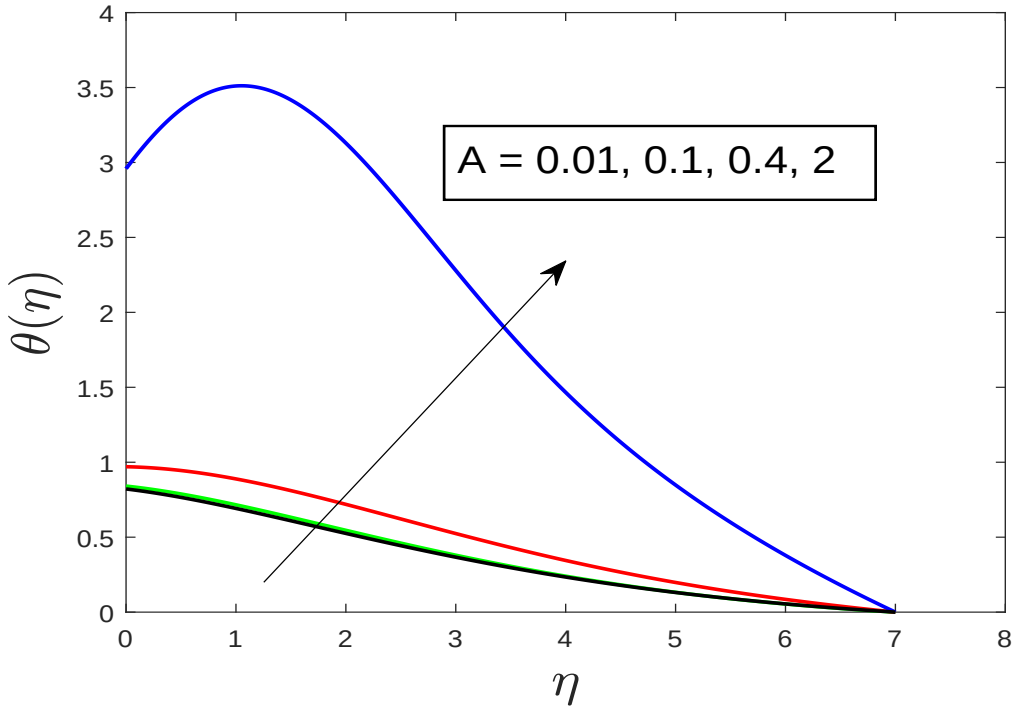

FIGURE 4.9: "Effect of A on $\theta(\eta)$ when $Nb = Nt = 0.5$, $Le = 2$, $\gamma = 0.1$, $Bi = 0.5$, $Pr = M = 1$, $Bi = 0.5$, $\delta = 0.2$, $R = 0.5$, $K = 0.5$, $Ec = 0.1$"

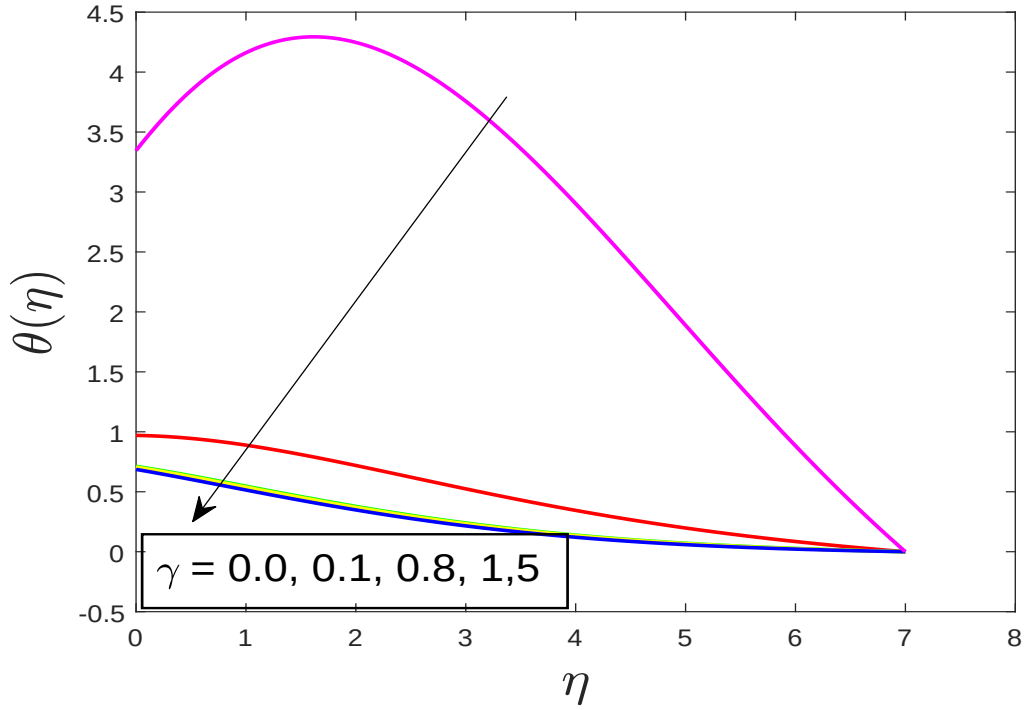

FIGURE 4.10: "Effect of γ on $\theta(\eta)$ when $Nb = Nt = 0.5$, $Le = 2$, $A = 0.4$, $Bi = 0.5$, $Pr = M = 1$, $\delta = 0.2$, $R = 0.5$, $K = 0.5$, $Ec = 0.1$

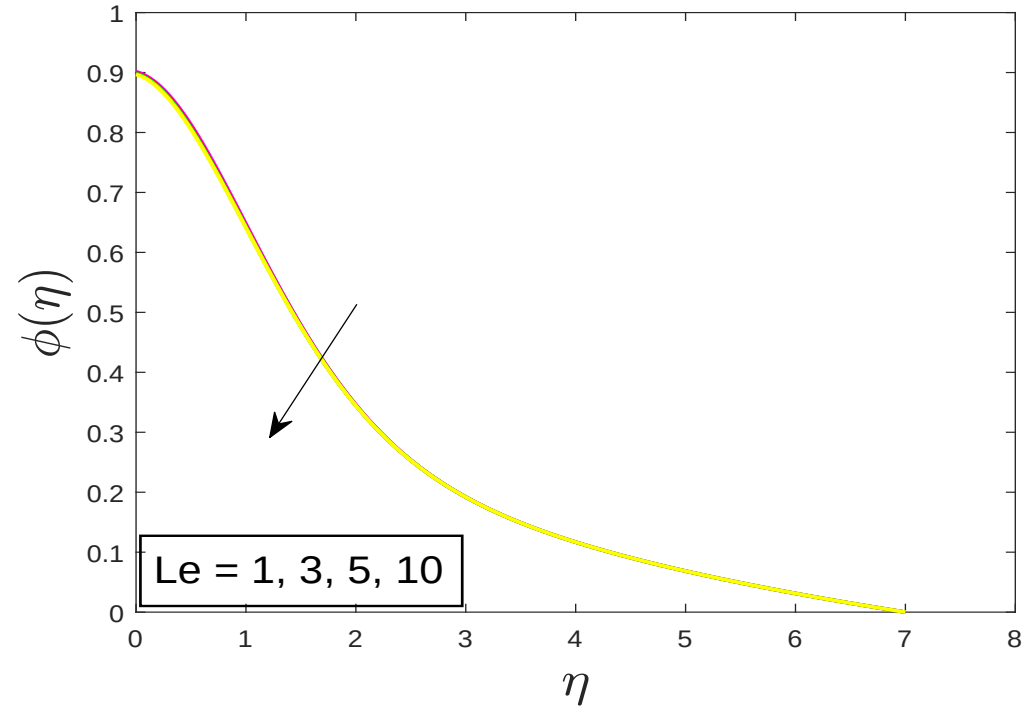

FIGURE 4.11: "Effect of Le on $\phi(\eta)$ when $Nb = Nt = Bi = 0.1$, $Pr = 5$, $A = 0.4$, $Bi = 0.5$, $M = 1$, $\delta = 0.1$, $\gamma = 0.2$, $R = 0.5$, $K = 0.5$, $Ec = 0.1$"

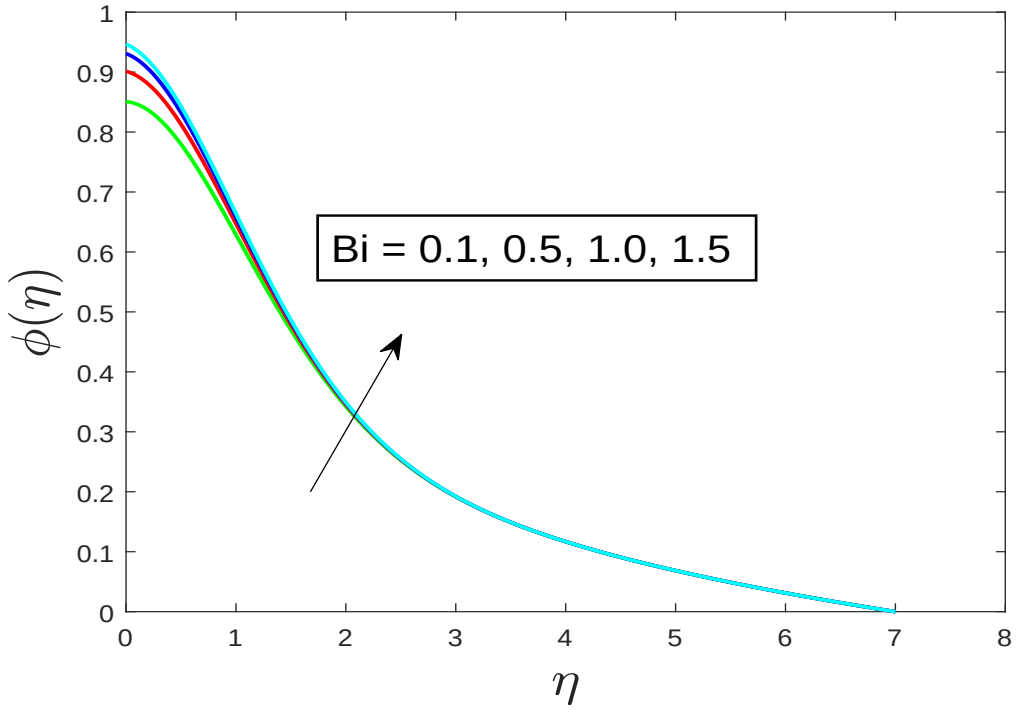

FIGURE 4.12: "Effect of Bi on $\phi(\eta)$ when $Nb = Nt = 0.1$, $Pr = 5$, $A = 0.4$, $M = 1$, $\delta = 0.1$, $\gamma = 0.2$, $R = 0.5$, $K = 0.5$, $Ec = 0.1$"

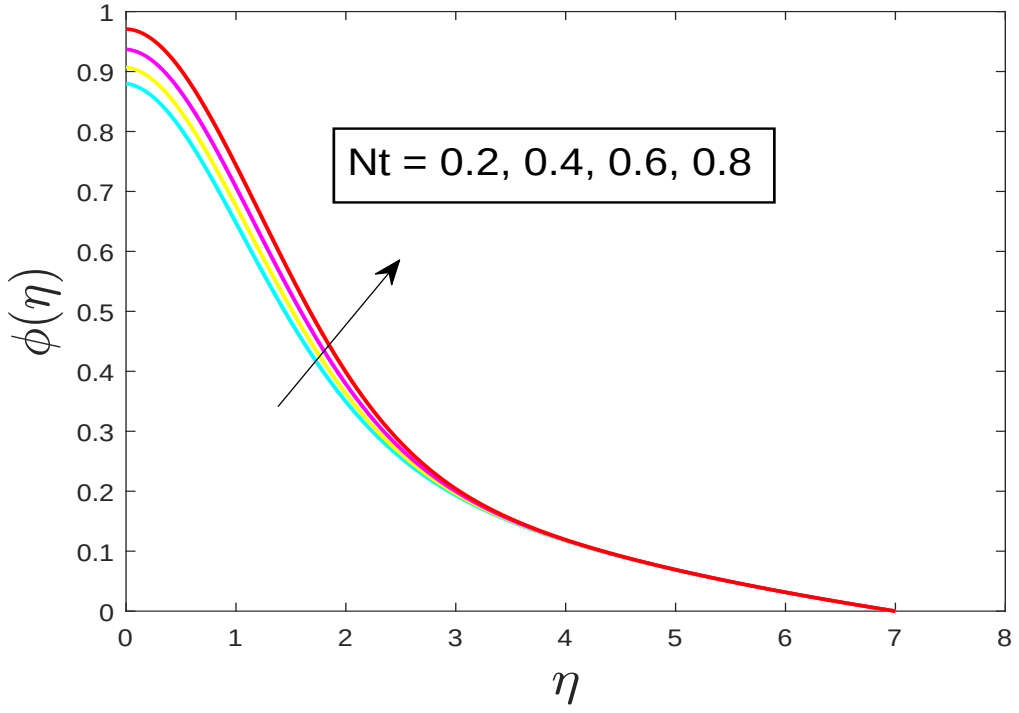

FIGURE 4.13: "Effect of Nt on $\phi(\eta)$ when $Nb = 0.1$, $Pr = 5$, $A = 0.4$, $M = 1$, $\delta = 0.1$, $Bi = \gamma = 0.2$, $R = 0.5$, $K = 0.5$, $Ec = 0.1$"

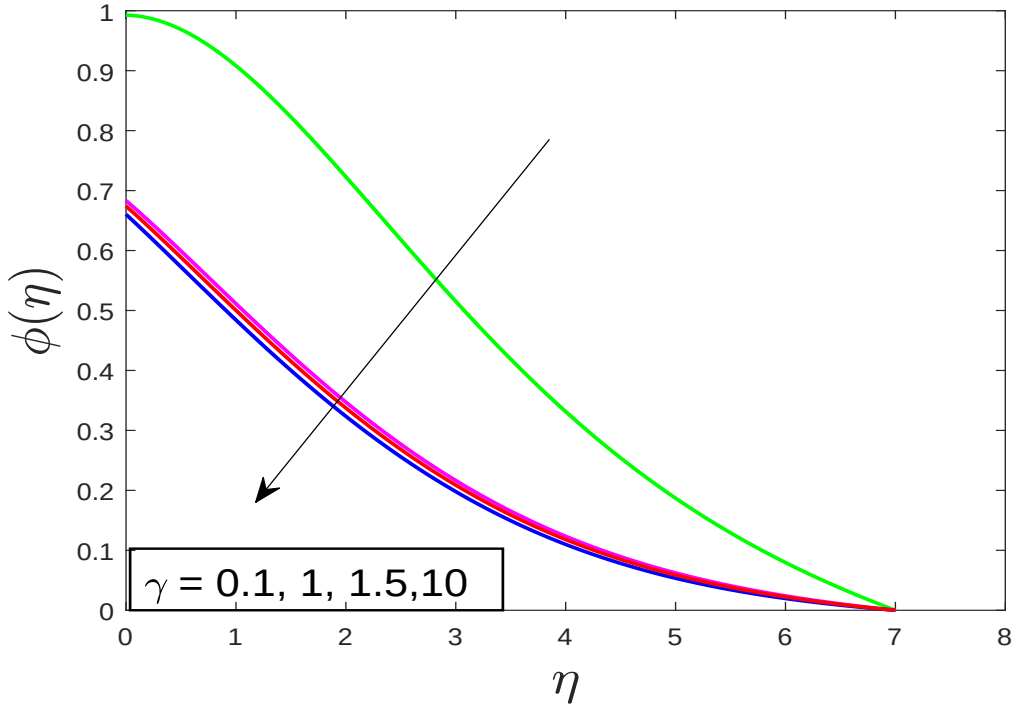

FIGURE 4.14: "Effect of γ on $\phi(\eta)$ when $Nb = Nt = 0.2$, $Le = 1$, $Bi = 0.5$, $\delta = 0.1$, $M = 1$, $A = 0.4$, $R = 0.5$, $k = 0.5$, $Ec = 0.1$"

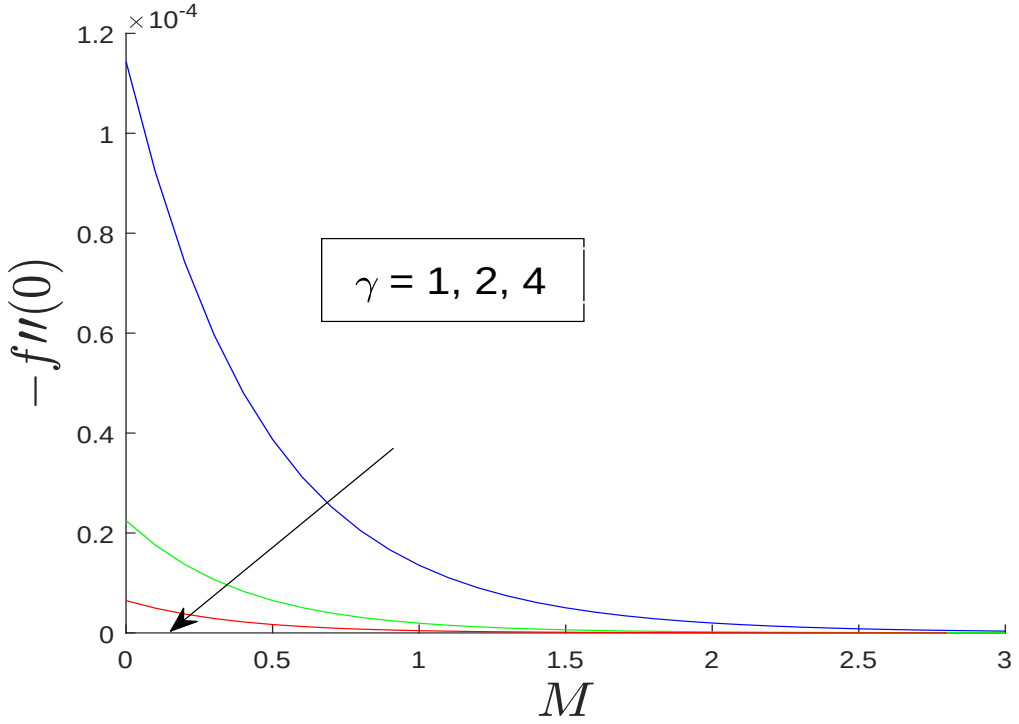

FIGURE 4.15: "Effect of γ on $-f''(0)$ when $Nb = Nt = 0.1$, $Le = 1$, $Pr = 2$, $\delta = 0.2$, $Bi = 10$, $A = 0.1$, $R = 0.5$, $k = 0.5$, $Ec = 0.1$"

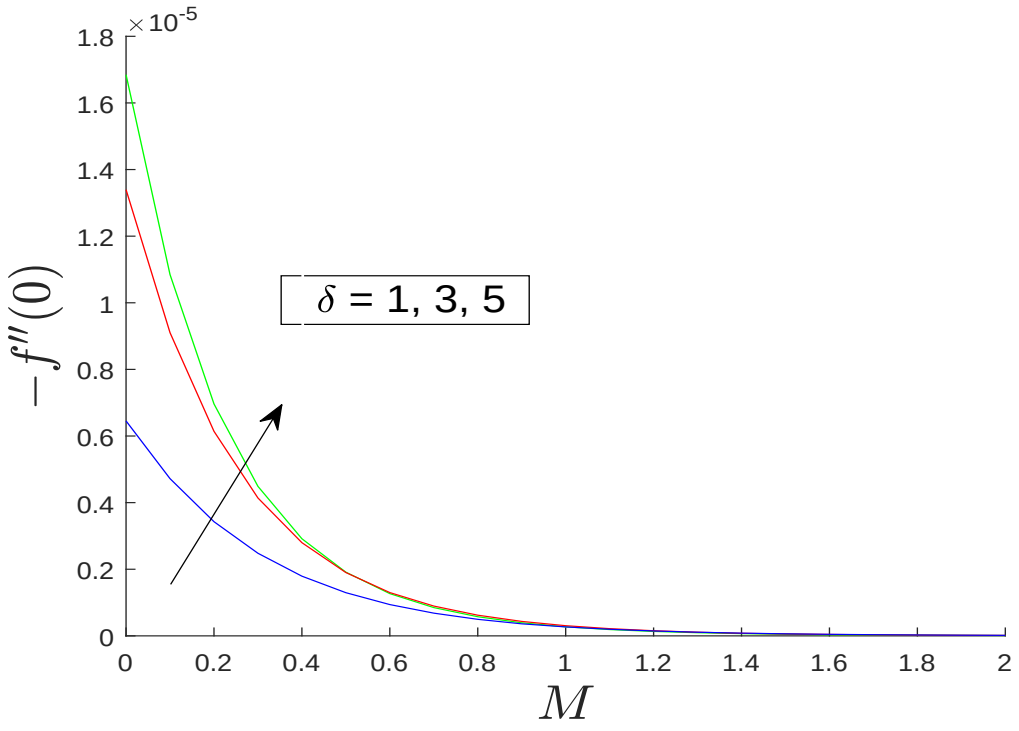

FIGURE 4.16: "Effect of δ on $-f''(0)$ when $Nb = Nt = 0.1$, $Le = 1$, $\gamma = 1$, $Pr = 2$, $A = 0.1$, $R = 0.5$, $k = 0.5$, $Ec = 0.1$"

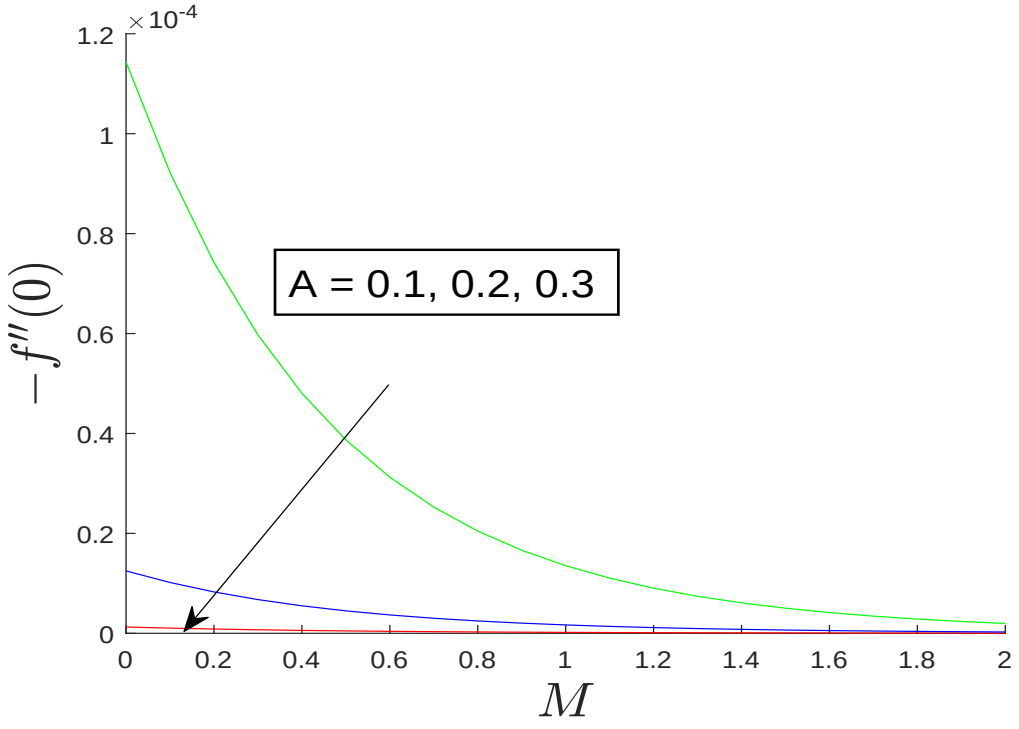

FIGURE 4.17: "Effect of A on $-f''(0)$ when $Nb = Nt = 0.1$, $Le = 2$, $\gamma = 1$, $\delta = 1$, $Pr = 2$, $Bi = 10$, $R = 0.5$, $k = 0.5$, $Ec = 0.1$"

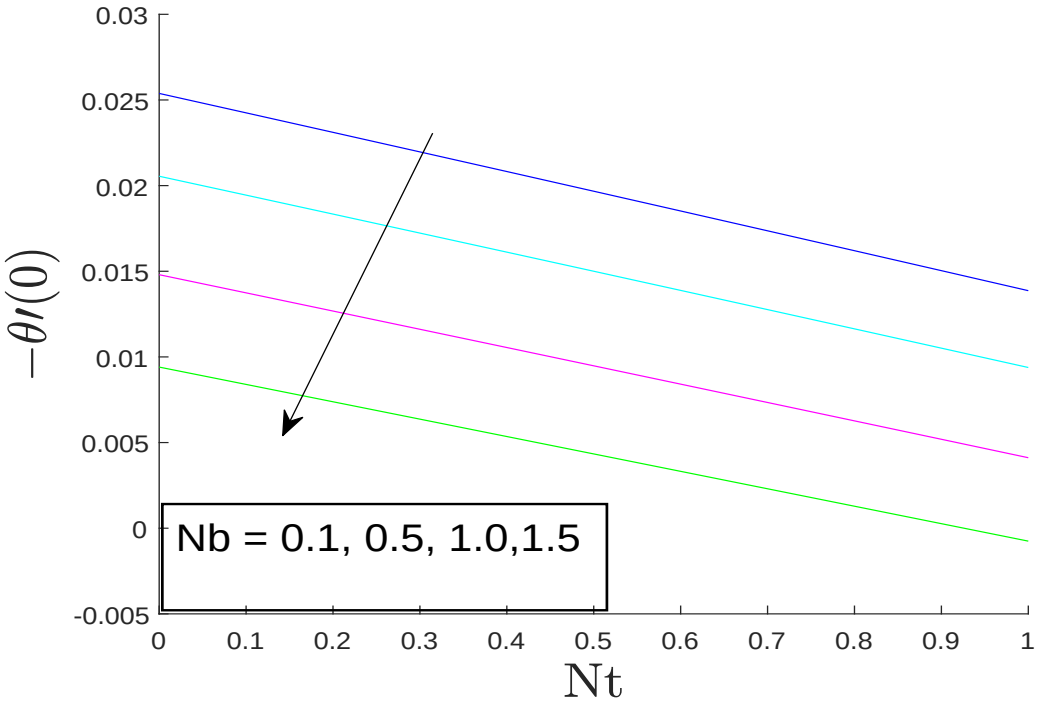

FIGURE 4.18: "Effect of Nb on $-\theta^{'}(0)$ when $Nt = 0.5$, $Le = 2$, $Bi = 0.5$, $\gamma = 0.1$, $\delta = 0.2$, $Pr = M = 1$, $A = 0.4$, $R = 0.5$, $k = 0.5$, $Ec = 0.1$"

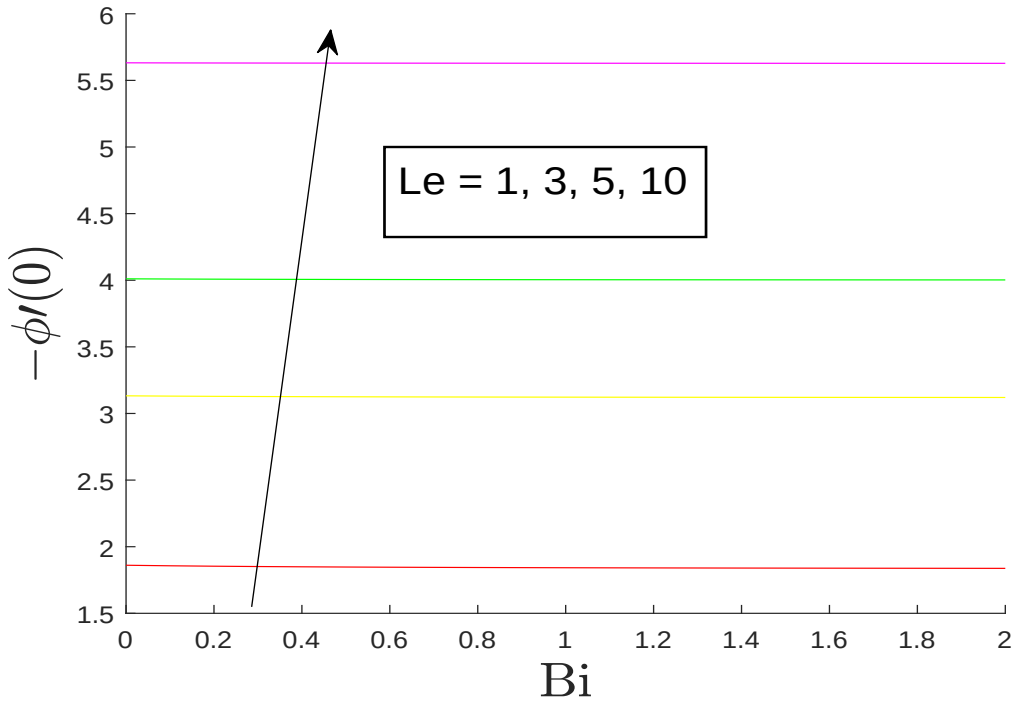

FIGURE 4.19: "Influence of Le on $-\phi^{'}(0)$ when $Nb = Nt = Bi = 0.1$, $Pr = 5$, $\gamma = 0.2$, $\delta = 0.1$, $M = 1$, $A = 0.4$, $R = 0.5$, $k = 0.5$, $Ec = 0.1$"

Chapter 5

Conclusion

Numerical investigation for the heat and mass transport of Casson nanofluid over a slip boundary and linear stretching sheet is presented in this thesis. The radiation and magnetic effects are also incorporated in this study. In addition to this, the effects of heat generation are also explored in the energy equation. Using appropriate similarity transformations, the conversion of non-linear partial differential equations describing the proposed flow problem to a set of ordinary differential equations was made. The shooting technique is employed for the numerical treatment. The impact of relevant flow parameters on the non-dimensional velocity, temperature and concentration profiles is illustrated in tabular and graphical forms. The main conclusions drawn from the numerical results are summarized below.

- The fluid velocity declines with increasing values of Casson and slip parameter.
- The fluid energy accelerates effectively with an increase in the Biot number.
- The temperature distribution enhances effectively with uprising values of Brownian motion and thermophoresis parameters.
- Concentration profile decelerates for the boosting values of Lewis number and thus we get a small molecular diffusivity and thermal boundary layer.

- Fluid concentration and associative boundary thickness are increasing functions of Casson parameter.
- It is noted that Nu_x is also increased by enhancing the values of Lewis number.

Bibliography

[1] S. Wang and W. Tan, "Stability analysis of double-diffusive convection of Maxwell fluid in a porous medium heated from below," *Physics Letters A*, vol. 372, no. 17, pp. 3046–3050, 2008.

[2] C. Fetecau and C. Nazar, "Unsteady flow of an Oldroyd-B fluid generated by a constantly accelerating plate between two side walls perpendicular to the plate," *International Journal of Non-linear Mechanics*, vol. 44, no. 10, pp. 1039–1047, 2009.

[3] R. Cortell, "Effects of viscous dissipation and work done by deformation on the MHD flow and heat transfer of a viscoelastic fluid over a stretching sheet," *Physics Letters A*, vol. 357, no. 4-5, pp. 298–305, 2006.

[4] M. Kothandapani and S. Srinivas, "Peristaltic transport of a Jeffrey fluid under the effect of magnetic field in an asymmetric channel," *International Journal of Non-Linear Mechanics*, vol. 43, no. 9, pp. 915–924, 2008.

[5] M. Jamil and C. Fetecau, "Some exact solutions for rotating flows of a generalized Burgers fluid in cylindrical domains," *Journal of Non-Newtonian Fluid Mechanics*, vol. 165, no. 23-24, pp. 1700–1712, 2010.

[6] M. M. Rashidi, M. M. Bhatti, M. A. Abbas, and M. E.-S. Ali, "Entropy generation on MHD blood flow of nanofluid due to peristaltic waves," *Entropy*, vol. 18, no. 4, p. 117, 2016.

[7] H. Alfvén, "Existence of electromagnetic-hydrodynamic waves," *Nature*, vol. 150, no. 3805, pp. 405–406, 1942.

[8] E. Witalis, "Hall magnetohydrodynamics and its applications to laboratory and cosmic plasma," *IEEE Transactions on Plasma science*, vol. 14, no. 6, pp. 842–848, 1986.

[9] S. Qian and H. H. Bau, "Magneto-hydrodynamics based microfluidics," *Mechanics research communications*, vol. 36, no. 1, pp. 10–21, 2009.

[10] O. Al-Habahbeh, M. Al-Saqqa, M. Safi, and T. A. Khater, "Review of magnetohydrodynamic pump applications," *Alexandria Engineering Journal*, vol. 55, no. 2, pp. 1347–1358, 2016.

[11] J. Bittencourt, "Simple applications of magnetohydrodynamics," in *Fundamentals of Plasma Physics*. Springer, 2004, pp. 299–324.

[12] A. Shahidian, M. Ghassemi, S. Khorasanizade, M. Abdollahzade, and G. Ahmadi, "Flow analysis of non-newtonian blood in a magnetohydrodynamic pump," *IEEE transactions on magnetics*, vol. 45, no. 6, pp. 2667–2670, 2009.

[13] P. Albano, C. Borghi, A. Cristofolini, M. Fabbri, Y. Kishimoto, F. Negrini, H. Shibata, and M. Zanetti, "Industrial applications of magnetohydrodynamics at the university of bologna," *Energy conversion and management*, vol. 43, no. 3, pp. 353–363, 2002.

[14] M. M. Rashidi, J. A. Esfahani, and M. Maskaniyan, "Applications of magnetohydrodynamics in biological systems-a review on the numerical studies," *Journal of Magnetism and Magnetic Materials*, vol. 439, pp. 358–372, 2017.

[15] K. Yih, "Free convection effect on MHD coupled heat and mass transfer of a moving permeable vertical surface," *International Communications in Heat and Mass Transfer*, vol. 26, no. 1, pp. 95–104, 1999.

[16] M. Modather and Chamkha, "An analytical study of MHD heat and mass transfer oscillatory flow of a micropolar fluid over a vertical permeable plate in a porous medium," *Turkish Journal of Engineering and Environmental Sciences*, vol. 33, no. 4, pp. 245–258, 2010.

[17] D. C. Kesavaiah, P. Satyanarayana, and S. Venkataramana, "Effects of the chemical reaction and radiation absorption on an unsteady MHD convective heat and mass transfer flow past a semi-infinite vertical permeable moving plate embedded in a porous medium with heat source and suction," *Int. J. of Appl. Math and Mech*, vol. 7, no. 1, pp. 52–69, 2011.

[18] L. Zheng, J. Niu, X. Zhang, and Y. Gao, "MHD flow and heat transfer over a porous shrinking surface with velocity slip and temperature jump," *Mathematical and Computer Modelling*, vol. 56, no. 5-6, pp. 133–144, 2012.

[19] M. A. Mahmoud and S. E. Waheed, "MHD stagnation point flow of a micropolar fluid towards a moving surface with radiation," *Meccanica*, vol. 47, no. 5, pp. 1119–1130, 2012.

[20] M. Mustafa, J. A. Khan, T. Hayat, and A. Alsaedi, "Sakiadis flow of Maxwell fluid considering magnetic field and convective boundary conditions," *Aip Advances*, vol. 5, no. 2, p. 027106, 2015.

[21] M. H. M. Yasin, A. Ishak, and I. Pop, "MHD stagnation-point flow and heat transfer with effects of viscous dissipation, Joule heating and partial velocity slip," *Scientific reports*, vol. 5, p. 17848, 2015.

[22] M. Sheikholeslami, D. D. Ganji, M. Y. Javed, and R. Ellahi, "Effect of thermal radiation on magnetohydrodynamics nanofluid flow and heat transfer by means of two phase model," *Journal of Magnetism and Magnetic Materials*, vol. 374, pp. 36–43, 2015.

[23] M. Chutia and P. Deka, "Numerical study on MHD mixed convection flow in a vertical insulated square duct with strong transverse magnetic field," *Journal of Applied Fluid Mechanics*, 2015.

[24] N. A. Kelson and A. Desseaux, "Effect of surface conditions on flow of a micropolar fluid driven by a porous stretching sheet," *International Journal of Engineering Science*, vol. 39, no. 16, pp. 1881–1897, 2001.

[25] W. Ibrahim and O. Makinde, "Magnetohydrodynamic stagnation point flow and heat transfer of Casson nanofluid past a stretching sheet with slip and convective boundary condition," *Journal of Aerospace Engineering*, vol. 29, no. 2, p. 04015037, 2016.

[26] R. W. Fox and A. T. Mcdonald, "Introduction to Fluid Mechanics," 2004.

[27] G. Bar-Meir, "Basics of Fluid Mechanics Version," *Chicago*, vol. 557, 2013.

[28] C. Kothandaraman, *Fundamentals of Heat and Mass Transfer*. New Age International, 2006.

[29] Y. A. Cengel, *Fluid Mechanics*. Tata McGraw-Hill Education, 2010.

[30] F. M. White and I. Corfield, *Viscous Fluid Flow*. McGraw-Hill New York, 2006, vol. 3.

[31] J. Kunes, *Dimensionless physical quantities in science and engineering*. Elsevier, 2012.

[32] A. J. Smits, *A Physical Introduction to Fluid Mechanics*. Wiley, 2000.

[33] J. D. Anderson and J. Wendt, *Computational fluid dynamics*. Springer, 1995, vol. 206.